1

2

3

4

5 **Onecut factors and Pou2f2 regulate the distribution of V2 interneurons in the**

6 **mouse developing spinal cord**

7

8 Audrey Harris[1], Gauhar Masgutova[1], Amandine Collin[1], Mathilde Toch[1], Maria

9 Hidalgo-Figueroa[1,4], Benvenuto Jacob[2], Lynn M. Corcoran[3], Cédric Francius[1,5] and Frédéric

10 Clotman[1*]

11

12 [1] Université catholique de Louvain, Institute of Neuroscience, Laboratory of Neural

13 Differentiation, Brussels, Belgium; [2] Université catholique de Louvain, Institute of

14 Neuroscience, System and Cognition division, Brussels, Belgium; [3] The Walter and Eliza Hall

15 Institute, Molecular Immunology Division and Immunology Division, Parkville, Victoria,

16 Australia.

17

18 **For correspondence** : frederic.clotman@uclouvain.be

19
20
21 [4] Present address : Neuropsychopharmacology & Psychobiology Research Group, Area of

22 Psychobiology, Department of Psychology, University of Cadiz, Spain; Instituto de

23 Investigación e Innovación en Ciencias Biomédicas de Cádiz (INiBICA), Spain

24 [5] Present address : PAREXEL International, France

25

26 Running title : Spinal interneuron migration

27

28 Key words : Embryonic spinal cord, V2 interneurons, Onecut, Pou2f2, neuronal migration,

29 differentiation

30

31

1

Abstract

Acquisition of proper neuronal identity and position is critical for the formation of neural circuits. In the embryonic spinal cord, cardinal populations of interneurons diversify into specialized subsets and migrate to defined locations within the spinal parenchyma. However, the factors that control interneuron diversification and migration remain poorly characterized. Here, we show that the Onecut transcription factors are necessary for proper diversification and distribution of the V2 interneurons in the developing spinal cord. Furthermore, we uncover that these proteins restrict and moderate the expression of spinal isoforms of *Pou2f2*, a transcription factor known to regulate B-cell differentiation. By gain- or loss-of-function experiments, we show that Pou2f2 contribute to regulate the position of V2 populations in the developing spinal cord. Thus, we uncovered a genetic pathway that regulates the diversification and the distribution of V2 interneurons during embryonic development.

Significance statement

In this study, we identify the Onecut and Pou2f2 transcription factors as regulators of spinal interneuron diversification and migration, two events that are critical for proper CNS development.

2

Introduction

Neuronal migration is a critical feature of CNS development. It enables neurons to reach an adequate location in the nervous parenchyma and to properly integrate into neural circuits. The mechanisms that regulate neuronal migration have been extensively studied in the developing brain, particularly for cortical interneurons (INs) (Barber and Pierani, 2016, Guo and Anton, 2014). In contrast, the factors that control IN migration in the developing spinal cord remain almost totally unknown.

In the embryonic spinal cord, distinct neuronal populations are generated from different progenitor domains orderly distributed along the dorso-ventral axis of the ventricular zone. These progenitors produce motor neurons and multiple populations of ventral or dorsal INs (Lai et al., 2016, Lu et al., 2015). Although spinal IN populations do not organize into columns along the anteroposterior axis of the spinal cord, they each migrate according to a stereotyped pattern and settle down at specific focused or diffuse locations in the spinal parenchyma (Grossmann et al., 2010). Recent studies demonstrated that proper neuronal distribution is critical for adequate formation of spinal circuits. Indeed, the clustering and dorso-ventral settling position of motor neuron pools critically pattern sensory input specificity (Surmeli et al., 2011). Position of dorsal INs along the medio-lateral axis in lamina V determines their connectivity with sensory afferents (Hilde et al., 2016) while extensor and flexor premotor INs segregate along the medio-lateral axis of the spinal cord (Tripodi et al., 2011). Positional distinctions among premotor INs additionally correlate with their output to different motor columns (Goetz et al., 2015) and differential distribution of V1 IN subsets constrain patterns of input from sensory and from motor neurons (Bikoff et al., 2016). Consistently, distinct ventral IN subsets are differentially distributed along the anteroposterior axis of the spinal cord (Bikoff et al., 2016, Francius et al., 2013, Hayashi et al., 2018) and integrate into specific local microcircuit modules (Hayashi et al., 2018). However, the molecular mechanisms that regulate proper distribution of spinal INs remain elusive.

During their migration, cardinal populations of spinal neurons undergo progressive diversification into distinct subsets that exert specific functions in spinal circuits (Catela et al., 2015, Lai et al., 2016, Lu et al., 2015). For example, V2 INs divide into major V2a and V2b and minor V2c and V2d populations characterized by the expression of Chx10, Gata3, Sox1 and Shox2, respectively. V2a and V2d are excitatory neurons that participate in left-right

84 alternation at high speed and contribute to rhythmic activation of locomotor circuits,
85 respectively (Crone et al., 2008, Dougherty and Kiehn, 2010, Dougherty et al., 2013). V2b
86 cells are inhibitory INs that participate in alternation of flexor vs extensor muscle contraction
87 (Britz et al., 2015). As observed for V1 INs (Bikoff et al., 2016), V2 cells further diversify into
88 more discrete subpopulations differentially distributed along the anteroposterior axis of the
89 spinal cord (Francius et al., 2013, Hayashi et al., 2018). However, specific functions of these
90 IN subsets have not been investigated yet, and the mechanisms that govern their production
91 remain currently unknown.

92 Recently, we identified Onecut (OC) transcription factors as regulators of neuronal
93 diversification (Kabayiza et al., 2017, Roy et al., 2012, Francius and Clotman, 2014) and of
94 dorsal IN migration (Kabayiza et al., 2017) in the developing spinal cord. OC factors, namely
95 Hepatocyte Nuclear Factor-6 (HNF-6, or OC-1), OC-2 and OC-3, are transcriptional activators
96 present in the digestive tract and in the CNS during embryonic development (Jacquemin et
97 al., 1999, Lemaigre et al., 1996, Jacquemin et al., 2003b, Landry et al., 1997, Vanhorenbeeck
98 et al., 2002). In neural tissue, they regulate production (Espana and Clotman, 2012a),
99 diversification (Roy et al., 2012, Francius and Clotman, 2014, Kabayiza et al., 2017),
100 distribution (Audouard et al., 2013, Espana and Clotman, 2012a, Espana and Clotman,
101 2012b, Kabayiza et al., 2017) and maintenance (Espana and Clotman, 2012a, Espana and
102 Clotman, 2012b, Stam et al., 2012) of specific neuronal populations, as well as the formation
103 of neuromuscular junctions (Audouard et al., 2012). Here, we demonstrate that OC factors
104 regulate the diversification and the distribution of V2 INs during spinal cord development.
105 Analyzes of OC-deficient embryos showed defective production of specific subpopulations of
106 V2a INs, as well as abnormal distribution of V2a and V2b cells in the developing spinal cord.
107 Furthermore, we uncovered that OC proteins act upstream of specific spinal isoforms of
108 Pou2f2, a POU family transcription factor. Using gain- or loss-of-function experiments, we
109 demonstrated that, as observed for OC factors, Pou2f2 regulates the distribution of V2 INs in
110 the developing spinal cord. Thus, we uncovered a genetic pathway that regulates the
111 diversification and the distribution of V2 INs during embryonic development.

112 **Results**

113

114 **OC factors are present in multiple subsets of spinal V2 INs**

115 In the developing spinal cord, OC factors contribute to diversification, migration and

116 maintenance of different neuronal populations (Kabayiza et al., 2017, Roy et al., 2012, Stam

117 et al., 2012). To study V2 IN diversification, we previously established a repertoire of

118 markers that divide embryonic V2 cells into multiple subpopulations (Francius et al., 2013).

119 Although OC factors have been detected in V2 INs (Francius and Clotman, 2010, Francius et

120 al., 2013) and are similarly distributed at distinct antero-posterior levels (Francius et al.,

121 2013), their production in V2 subsets has not been investigated yet. Therefore, we first

122 determined the presence of each OC in these V2 subpopulations at e12.5.

123 V2a INs include neuronal subsets characterized by the presence of Shox2, MafA, cMaf,

124 Bhlhb5 or Prdm8 (Francius et al., 2013). Only Hnf6 was detected in few Shox2+ V2a cells

125 (Figure 1A-C"; Table 1). In contrast, the 3 OC proteins were detected in MafA+ and cMaf+

126 V2a subpopulations (Figure 1D-I"; Table 1), but not in Bhlhb5+ or Prdm8+ cells (Table 1; data

127 not shown). V2b INs include similar subsets except for Shox2+ and cMaf+ cells, and contain

128 an additional MafB+ subpopulation (Francius et al., 2013). OC were present in MafA+ but not

129 in MafB+, Bhlhb5+ or Prdm8+ V2b subsets (Figure 1J-L"; Table 1; data not shown). In

130 addition, OC were detected in V2c (non-progenitor Sox1+ cells; Figure 1M-O"; Table 1) but

131 not in V2d (Shox2+Chx10-) cells (Figure 1A-C"; Table 1). Thus, OC factors are present in

132 multiple subpopulations of V2 INs.

133

134 **OC factors regulate the diversification of spinal V2 INs**

135 To determine whether OC proteins contribute to the development of V2 IN subsets, we

136 characterized the phenotype of these cells in *Hnf6/Oc2* double-mutant embryos, which lack

137 the three OC factors in the developing spinal cord (Kabayiza et al., 2017, Roy et al., 2012).

138 Given that the number and the distribution of cells in each IN subpopulation vary along the

139 anteroposterior axis of the spinal cord (Francius et al., 2013, Hayashi et al., 2018, Sweeney et

140 al., 2018), this analysis was systematically performed at brachial, thoracic and lumbar levels

141 at e12.5 and e14.5.

142 In the absence of OC factors, the total number of Chx10+ INs was not significantly changed

143 (Figure 2A-D; Supplementary Figure S1A-B), although a trend toward reduction was detected

144   at brachial level at e12.5 (Figure 2C). Consistently, the number of Chx10+Shox2+ INs was not

145   changed (Figure 2E-H; Supplementary Figure S1C-D"). These observations suggest that OC

146   are not necessary for V2a IN production. In contrast, the smaller V2a subpopulations

147   wherein OC factors were detected in control embryos, characterized by the presence of

148   MafA (Figure 1D-F") or cMaf (Figure 1G-I"), were almost completely lost in OC mutant

149   embryos (Figure 2I-P; Supplementary Figure S1E-H"). As the total number of Chx10+ and of

150   Shox2+ V2a was not changed (Figure 2A-H; Supplementary Figure S1A-D"), the loss of the

151   MafA+ or cMaf+ subsets may be compensated for by expansion of other V2a

152   subpopulations, markers of which remain to be identified. Nevertheless, our data indicate

153   that OC factors are required either for the expression of V2 subpopulation markers or for the

154   differentiation of specific V2a IN subsets.

155   To discriminate between these possibilities and to evaluate the contribution of OC factors to

156   V2b diversification, we characterized the phenotype of V2b INs and of their MafA+

157   subpopulation in the absence of OC proteins. As observed for V2a INs, the total number of

158   V2b cells was not changed in OC mutant embryos (Figure 2Q-T; Supplementary Figure S1I-J),

159   although a trend toward reduction was observed at brachial level at e12.5 (Figure 2S).

160   However, in contrast to V2a, the MafA+ V2b INs were present in normal number in OC

161   mutant embryos (Figure 2U-X; Supplementary Figure S1K-L''). Hence, OC factors are not

162   necessary for the production of the MafA+ V2b subset, although they are required for

163   proper differentiation of the MafA+ and of the cMaf+ V2a subpopulations.

164   Finally, we assessed the requirement for OC in the production of V2c INs, a V2 population

165   strongly related to V2b cells (Panayi et al., 2010). Although weak production of Sox1 in spinal

166   progenitors was preserved, V2c cells characterized by high Sox1 levels were scarcely

167   detectable in OC mutant embryos at e12.5 (arrows in Figure 2Y-AA). However, the number

168   of V2c was normal at e14.5 (Figure 2BB; Supplementary Figure S1M-N), suggesting that the

169   absence of OC delays the differentiation of V2c INs without affecting the V2b population.

170   Taken together, these observations demonstrate that OC proteins are not required for V2 IN

171   production but regulate the diversification of V2 INs into multiple subpopulations.

172

173   **OC factors regulate the distribution of spinal V2 INs**

174   Although the total number of V2a or V2b INs was not affected by the absence of OC factors,

175   careful examination of immunofluorescence labelings suggested that, as observed for spinal

176   dorsal INs (Kabayiza et al., 2017), OC proteins may regulate the distribution of V2 INs in the

177   developing spinal cord (Figure 2A-B; Q-R). Therefore, quantitative distribution analyses

178   (Kabayiza et al., 2017) were performed for each V2 population at brachial, thoracic or

179   lumbar levels at e12.5, namely in the course of ventral IN migration, and at e14.5, i.e. when

180   ventral IN migration in the transverse plane of the spinal cord is completed. Absence of the

181   MafA+ and cMaf+ V2a subpopulations in OC mutants and the small size of other V2 subsets

182   prevented analysis of subpopulation distribution.

183   At e12.5 in control embryos, V2a INs distributed in 2 connected clusters, a major central

184   group and a minor medial group, at each level of the spinal cord (Figure 3A-C). In mutant

185   embryos, V2a cells similarly distributed in connected central and medial groups. However,

186   the relative cell distribution between the 2 clusters was altered, with less central cells at

187   brachial level and less medial cells at lumbar levels (Figure 3D-L). Altered V2a distribution on

188   the medio-lateral axis was confirmed at e14.5. In control embryos, the 2 V2a groups did

189   coalesce in a more evenly-distributed population that occupied ~70% of the medio-lateral

190   axis (Figure 3M-O). In mutant embryos, V2a INs remained segregated into 2 distinct,

191   although connected, clusters with a majority of cells in medial position (Figure 3P-X). Thus,

192   absence of OC factors perturbs proper distribution of the V2a INs and restricts at e14.5

193   migration of a fraction of V2a cells in a medial position.

194   To assess whether OC also regulate the position of other V2 populations, we studied the

195   distribution of V2b INs. At e12.5 in control embryos, V2b cells distributed in a major central

196   (brachial level) or lateral (thoracic and lumbar levels) cluster with minor subsets located

197   more medially (arrows in Figure 4A-C) or ventrally (arrowheads in Figure 4A-C). In OC mutant

198   embryos at e12.5, the major population was more compact, more centrally located and

199   slightly more ventral. In addition, the ventral V2b subset was significantly depleted (Figure

200   4P-X). Consistently, at e14.5, V2b INs in the central cluster remained significantly more

201   compact at thoracic level in the absence of OC factors, and identical trends were observed at

202   brachial and lumbar levels (Figure 4M-X). In addition, a small contingent of V2b migrating

203   towards the medio-dorsal spinal cord in control embryos (arrowheads in Figure 4N,O) was

204   missing in OC mutant littermates (Figure 4Q-X). Taken together, these observations

205   demonstrate that, in addition to V2 diversification, the OC transcription factors regulate

206   proper distribution of V2 INs during spinal cord development.

207

208 **OC factors control expression of neuronal-specific isoforms of *Pou2f2***

209 To identify genes downstream of OC that may contribute to V2 IN differentiation and

210 distribution, we performed a microarray comparison of control and of OC-deficient spinal

211 cord transcriptome at e11.5, namely at the stage when significant numbers of V2 cells have

212 been generated and are initiating migration (GEO repository accession number: GSE117871).

213 Among genes showing a differential expression level in the OC mutant spinal cord, *Pou2f2*

214 was significantly upregulated (1.57-fold increase). Pou2f2 (previously named Oct-2) is a

215 transcription factor containing a POU-specific domain and a POU-type homeodomain (Figure

216 5A) that binds an octamer motif (consensus sequence ATGCAAAT) (Latchman, 1996). *Pou2f2*

217 expression has been detected in B lymphocytes, in neuronal cell lines and in neural tissues

218 including the developing CNS (Lillycrop and Latchman, 1992, Camos et al., 2014, Hatzopoulos

219 et al., 1990). Pou2f2 is required for differentiation of B lymphocytes and for postnatal

220 survival (Corcoran et al., 1993, Corcoran et al., 2004, Hodson et al., 2016, Konig et al., 1995),

221 and is able to modulate neuronal differentiation of ES cells (Theodorou et al., 2009).

222 However, its role in the developing spinal cord remains unknown.

223 Based on work in B cells, multiple *Pou2f2* isoforms generated by alternative splicing have

224 been described (Figure 5A; (Lillycrop and Latchman, 1992, Wirth et al., 1991, Hatzopoulos et

225 al., 1990, Liu et al., 1995, Stoykova et al., 1992)). Therefore, we first determined whether

226 similar isoforms are found in the developing spinal cord. However, we systematically failed

227 to obtain RT-PCR products using upstream primers in described exon 1 (asterisks in

228 Supplementary Figure S2A-B and data not shown; Table 2) and amplifications encompassing

229 exons 5 to 6 generated predominant amplicons larger than expected (arrowheads in

230 Supplementary Figure S2B; Table 2), suggesting the existence of alternative exons in *Pou2f2*

231 embryonic spinal cord transcripts (Figure 5A). Data mining the NCBI Nucleotide database for

232 *Pou2f2* sequences identified a predicted murine *Pou2f2* isoform (X6 sequence, accession

233 number XM_006539651.3) with a different exon 1 (E1X) and an additional sequence

234 between exons 5 and 6, the size of which (279 bp) corresponded to the size differences

235 estimated in our amplifications encompassing exons 5 to 6 (arrowheads in Supplementary

236 Figure S2B; Table 2). Using PCR primers in this predicted sequence, we were able to amplify

237 a 5' region of *Pou2f2* from the alternative E1X exon and an additional sequence between

238 exons 5 and 6 (Supplementary Figure S2C; Table 2), suggesting that alternative isoforms

239 similar to this predicted sequence are produced in the developing spinal cord. However,

240 amplifications from E1X systematically produced 2 amplicons (arrowheads in Supplementary

241 Figure S2C; Table 2), suggesting the existence of an alternative exon downstream to E1X.

242 Sequencing of our PCR products and alignment to genomic DNA confirmed that

243 predominant *Pou2f2* isoforms in the developing spinal cord contain the alternative E1X exon,

244 an additional exon (E5b) between exons 5 and 6, and can undergo alternative splicing of a

245 short (61bp) exon (E1b) between E1X and exon 2 (Supplementary Figure S2D). E5b exon

246 maintains the reading frame. In contrast E1b exon disrupts it, imposing the use of the ATG

247 located in exon 2 to generate a functional Pou2f2 protein, whereas the absence of E1b

248 leaves open the use of an alternative upstream ATG located at the 3' end of E1X (Figure 5A;

249 Supplementary Figure S2D). Hence, our RT-PCR and sequencing data indicate that 4

250 neuronal *Pou2f2* isoforms different from the previously described B-cell or neural isoforms

251 are produced in the developing spinal cord (Figure 5A).

252 However, minor transcripts corresponding to B-cell isoforms are also detected in the

253 embryonic spinal cord (Supplementary Figure S2A-B; Table 2). To assess the relative

254 abundance of each transcript type in this tissue and to evaluate the extent of their relative

255 overexpression in the absence of OC factors, we quantified each isoform type in control and

256 in OC-deficient spinal cord at e11.5. In control spinal cords, spinal *Pou2f2* isoforms were >30-

257 fold more abundant than B-cell isoforms (Figure 5B), consistent with our RT-PCR

258 observations (Supplementary Figure S2). In the absence of OC factors, spinal isoforms were

259 ~2.6-fold overexpressed whereas B-cell isoforms barely trended to increase (Figure 5C-E).

260 Thus, OC factors repress expression of spinal *Pou2f2* isoforms in the developing spinal cord.

261 To confirm these data and to determine the expression pattern of *Pou2f2* in the ventral

262 spinal cord, *in situ* hybridization was performed on sections from control or *Hnf6/Oc2*

263 double-mutant spinal cords using either a generic *Pou2f2* probe complementary to spinal

264 and to B-cell isoforms or a spinal isoform-specific probe corresponding only to exon E5b

265 (Figure 5A). Using the generic *Pou2f2* probe on control tissue, we detected *Pou2f2*

266 transcripts in the ventral region of the spinal cord, with lower expression levels in the

267 location of the motor columns (arrows in Figure 5F). In OC mutant embryos, *Pou2f2*

268 expression was globally increased and additionally expanded in the ventral area (arrowheads

269 in Figure 5F-G) including the motor neuron territories (arrows in Figure 5F-G). Similar

270 observations were made with the spinal isoform-specific probe (Figure 5H-I). Thus, OC

271 factors restrict and moderate *Pou2f2* expression in ventral spinal populations likely including

272 V2 INs.

273

Pou2f2-positive V2 INs are mislocated in the absence of OC factors

275 To assess whether increased *Pou2f2* expression in *Hnf6$^{-/-}$;Oc2$^{-/-}$* spinal cords corresponded to

276 an expansion of Pou2f2 distribution in V2 INs or an upregulation in its endogenous

277 expression territory, we first quantified the number and distribution of Pou2f2-containing

278 Chx10+ cells at e12.5 and e14.5 (Figure 6; Supplementary Figure S3). Immunofluorescence

279 experiments demonstrated that Pou2f2 is present in V2a INs in control embryos (Figure

280 6A,C; Supplementary Figure S3A,D), although it was only sparsely detected in MafA+ and

281 cMaf+ V2a subsets (data not sown). Intensity of the labeling confirmed increased Pou2f2

282 production in the ventral regions of the spinal cord in OC mutant embryos (Figure 6A-F).

283 However, the number in Pou2f2-positive V2a INs was not significantly different (Figure 6E-F;

284 Supplementary Figure S3), suggesting that Pou2f2 is increased in its endogenous expression

285 domain. In contrast, the distribution of Pou2f2-positive V2a INs was affected (Figure 6A-D,

286 6G-DD). At e12.5, cells in the central clusters were slightly reduced at brachial and at

287 thoracic levels (Figure 6G-R). In contrast, at e14.5, a majority of V2a containing Pou2f2

288 settled in a medial position (Figure 6S-DD), reminiscent of the distribution defects observed

289 for the whole V2a population (Figure 3). Similarly, Pou2f2 was detected in V2b INs in control

290 embryos, although in a more restricted number of cells (Figure 7A-B, E). In the absence of OC

291 factors, the number of Pou2f2-positive V2b cells was not significantly increased (Figure 7E-F)

292 but, as observed for V2a, this subset of V2b INs was mislocated with cells more central at

293 e12.5 and more clustered on the medio-lateral axis at e14.5 (Figure 7G-DD). Taken together,

294 these observations suggest that Pou2f2 may contribute to control V2 IN migration during

295 spinal cord development and could participate in alterations of V2 distribution in the

296 absence of OC factors.

297

Pou2f2 regulates the distribution of spinal V2 INs

299 To determine whether Pou2f2 is able to modulate V2 IN distribution, we overexpressed

300 *Pou2f2* in the chicken embryonic spinal cord (Supplementary Figure S4). Increased Pou2f2

301 did not impact on the number of V2a or V2b (Figure 8A-F). In contrast, it did alter V2 IN

302 location. In HH27-28 control spinal cord, V2a INs were distributed in 2 closely connected

303   clusters on the medio-lateral axis of the neuroepithelium (Figure 8G). In electroporated

304   spinal cord, lateral migration was increased and a majority of V2a INs were clustered in a

305   single group in a central position (Figure 8H-J) with ectopic lateral extensions (arrow in

306   Figure 8H). In control spinal cord, V2b were distributed in 2 groups along the medio-lateral

307   axis with a majority of cells in the lateral cluster (Figure 8K). In electroporated spinal cord,

308   the V2b INs were equally distributed between these 2 clusters (Figure 8L-N). Thus, consistent

309   with our observation in OC mutant embryos, increased Pou2f2 can modulate the distribution

310   of V2 INs in the developing spinal cord.

311   To confirm the influence of Pou2f2 on V2 migration, we studied V2 distribution in mouse

312   embryos devoid of Pou2f2 (Corcoran et al., 1993) at e12.5. Absence of Pou2f2 did not impact

313   on the number of V2a INs (Figure 9A-C) nor on the Shox2+, cMaf+ or MafA+ V2a subsets

314   (Supplementary Figure S5). In contrast, V2a distribution was affected in *Pou2f2* mutants. As

315   compared to the two V2a clusters observed in control embryos, Chx10+ cells were more

316   scattered in *Pou2f2* mutant embryos (Figure 9D-O). Furthermore, although the number of

317   V2b, V2c or MafA+ V2b cells was not changed in the absence of Pou2f2 (Figure 10A-C;

318   Supplementary Figure S6), V2b cells remained more medial at brachial and thoracic levels

319   and segregated more extensively on the medio-lateral axis at lumbar levels (Figure 10D-O).

320   Taken together, these observations demonstrate that Pou2f2 regulate the distribution of V2

321   INs during spinal cord development.

322

Discussion

In the recent years, several studies demonstrated that proper distribution of neuronal populations and subpopulations in the developing spinal cord is critical for adequate formation of spinal circuits (Bikoff et al., 2016, Goetz et al., 2015, Hayashi et al., 2018, Hilde et al., 2016, Surmeli et al., 2011, Tripodi et al., 2011). However, the genetic programs that control the diversification of spinal neuronal populations into specialized subpopulations and the proper settling of these neuronal subsets in the spinal parenchyma remain elusive. Here, we provide evidence that OC transcription factors regulate the diversification of spinal V2 INs, and that a genetic cascade involving OC factors and their downstream target Pou2f2 controls the distribution of V2 INs in the developing spinal cord.

Control of V2 IN diversification by the OC factors

Cardinal populations of spinal ventral INs have been well characterized, and their global contribution to the activity of motor circuits has been extensively studied (reviewed in (Boije and Kullander, 2018, Gosgnach et al., 2017, Ziskind-Conhaim and Hochman, 2017). However, more recently, the idea emerged that these cardinal populations are not homogeneous ensembles but rather contain multiple neuronal subsets with distinct molecular identities and functional properties (Bikoff et al., 2016, Borowska et al., 2015, Borowska et al., 2013, Francius et al., 2013, Sweeney et al., 2018, Talpalar et al., 2013). V2a INs comprise two major divisions, namely type I and type II V2a cells, that are arrayed in counter-gradients along the antero-posterior axis of the spinal cord and activate different patterns of motor output at brachial or lumbar levels. Furthermore, these two large divisions can themselves be fractionated at birth into 11 subsets characterized by distinct combinations of markers, differential segmental localization and specific distribution patterns on the medio-lateral axis of the spinal cord (Hayashi et al., 2018). In the zebrafish, 3 distinct subclasses of V2a INs participate in separate microcircuit modules driving slow, intermediate or fast motor neuron activity (Ampatzis et al., 2014). Taken together, these observations suggest that cardinal IN populations only constitute the first organization level of functionally distinct neuronal subsets that contribute to diversity and flexibility within spinal motor circuits.

We showed here that OC factors are present in subsets of V2 INs and contribute to their diversification. Normal numbers of cardinal V2a and V2b cells were generated in OC mutant embryos, suggesting that these factors do not contribute to the production of V2 cells (Clovis

355   et al., 2016, Lee et al., 2008, Thaler et al., 2002) nor to the segregation of the V2a and V2b

356   lineages through differential activation of Notch signaling (Del Barrio et al., 2007, Joshi et al.,

357   2009, Misra et al., 2014, Peng et al., 2007). In contrast, V2a subpopulations characterized by

358   the presence of MafA or cMaf were strongly depleted in the absence of OC proteins. This

359   observation results either from a loss of these V2a subsets or from a downregulation of

360   *MafA* or *cMaf* expression in these cells. Uncomplete knowledge of the whole collection of

361   V2a subsets prevented to assess whether this apparent loss of specific subpopulations was

362   compensated for by an expansion of neighboring subsets. Nevertheless, these data

363   demonstrate altered differentiation of V2 IN subsets in the absence of OC factors, as

364   previously observed for spinal motor neurons (Roy et al., 2012) and dorsal INs (Kabayiza et

365   al., 2017). In addition, the production of V2c cells was delayed in OC mutant embryos,

366   although V2b that are supposed to constitute the source of V2c (Panayi et al., 2010) were

367   timely generated. This points to a specific contribution of OC protein to the development of

368   V2c INs, the mechanism of which is currently unknown.

369

370   **Control of V2 IN distribution by the OC factors**

371   Beside diversification, the characterization of functionally distinct IN subpopulations

372   unveiled a strong correlation between the distribution of each IN subset and their

373   contribution to distinct microcircuit modules (Bikoff et al., 2016, Borowska et al., 2013,

374   Goetz et al., 2015, Hayashi et al., 2018, Hilde et al., 2016, Tripodi et al., 2011). These data

375   support a model wherein correct localization of spinal IN subsets is critical for proper

376   formation of sensory and sensory-motor circuits, highlighting the importance of a strict

377   regulation of short-distance neuronal migration in the developing spinal cord. However,

378   genetic determinants that control spinal IN migration have only been sparsely identified.

379   Sim1 regulate ventro-dorsal migration of the V3 IN subsets (Blacklaws et al., 2015). Similarly,

380   SATB2 control the position of inhibitory sensory relay INs along the medio-lateral axis of the

381   spinal cord (Hilde et al., 2016). Here, we provide evidence that the OC factors control a

382   genetic program that regulates proper positioning of V2 INs during embryonic development.

383   In the absence of OC proteins, a fraction of V2a INs remained in a more medial location,

384   expanding the medial cluster containing locally-projecting cells at the expanse of the lateral

385   cluster that comprises the supraspinal-projecting V2a INs (Hayashi et al., 2018). V2b

386   alterations were less spectacular, although ventral and dorsal contingents were reduced and

387 the cell distribution in the central cluster was altered. Variability in the alterations observed

388 at e12.5 and e14.5 highlights that spinal migration is not completed at e12.5 and suggests

389 that distribution of earlier- or later-migrating neurons may be differently affected by the

390 absence of OC proteins. In addition, migration along the anteroposterior axis, which can not

391 be analyzed in our experimental setup, could also be perturbed. Alterations of the

392 distribution of V2a and V2b interneurons likely correlate with alterations in their

393 differentiation program. Indeed, the production of adequate clues to ensure proper cell

394 positioning is an intrinsic component of any neuronal differentiation program (Blacklaws et

395 al., 2015, Hayashi et al., 2018, Hilde et al., 2016). In any case, our observations are consistent

396 with the contribution of OC factors to the migration of several populations of spinal dorsal

397 INs (Kabayiza et al., 2017). This raises the question whether similar cues might be regulated

398 by identical genetic programs and used by different IN populations to organize proper

399 distribution of ventral and dorsal IN subsets in the developing spinal cord. Identification of

400 the factors downstream of OC protein involved in the control of neuronal migration will be

401 necessary to answer this question.

402

403 **An OC-Pou2f2 genetic cascade regulates the migration of V2 INs**

404 Therefore, we attempted to identify genes downstream of OC factors and possibly involved

405 in the control of IN migration using a global approach comparing the transcriptome of whole

406 spinal cords isolated from control or OC-deficient embryos. Absence of known regulators of

407 neuronal migration among the most affected genes suggests that different actors may be

408 active downstream of OC proteins in distinct IN populations to regulate proper neuronal

409 distribution. In contrast, we uncovered that expression of the transcription factor *Pou2f2* is

410 repressed by OC factors in different spinal populations. Surprisingly, our data demonstrated

411 that variant *Pou2f2* isoforms are produced in the developing spinal cord as compared to B

412 lymphocytes (Lillycrop and Latchman, 1992, Wirth et al., 1991, Hatzopoulos et al., 1990, Liu

413 et al., 1995, Stoykova et al., 1992), and that these spinal variants are regulated by OC

414 proteins. Spinal-enriched transcripts encode Pou2f2 proteins containing additional peptidic

415 sequences upstream of the POU-specific domain and of the homeodomain. Furthermore,

416 exon 1 is different and corresponds to sequences located ~47kb upstream of the

417 transcription initiation site used in B cells (data not shown) in the mouse genome, suggesting

418 that OC regulate *Pou2f2* expression from an alternative promoter. However, we cannot

14

419   exclude that additional exon(s) could be present upstream of the identified sequences, and

420   determination of the regulating sequences targeted by the OC protein will require thorough

421   characterization of the produced transcripts. In addition, we cannot rule out indirect

422   regulation of *Pou2f2* expression by the OC factors, as OC are usually considered to be

423   transcriptional activators rather than repressors (Beaudry et al., 2006, Jacquemin et al.,

424   2000, Jacquemin et al., 2003a, Lannoy et al., 2000, Pierreux et al., 2004, Roy et al., 2012).

425   Nevertheless, our observations demonstrate that Pou2f2 is downstream of OC factors in the

426   V2 INs and also contributes to regulate the distribution of V2 INs during embryonic

427   development. The number of Pou2f2-containing V2 was not significantly increased in OC

428   mutant spinal cords, suggesting that the absence of OC protein resulted in relaxing of Pou2f2

429   production in its endogenous expression domain rather that ectopic activation in other V2

430   subsets. Increased production of Pou2f2 in the chicken embryonic spinal cord resulted in

431   alterations in the localization of V2 populations without any change in cell number, pointing

432   to a possible contribution of Pou2f2 to the regulation of V2 migration downstream of OC

433   factors. Consistently, V2 distribution was perturbed in *Pou2f2* mutant embryos without any

434   alteration in V2 population or subpopulation cell numbers, demonstrating the involvement

435   of Pou2f2 in the control of V2 IN distribution. Alterations in V2 distribution after *Pou2f2*

436   electroporation were not comparable to that observed in OC mutant embryos and were not

437   strictly opposite to *Pou2f2* knockout phenotype because the developmental stages obtained

438   after chicken embryo electroporation were much earlier than the developmental stages of

439   analyzed mouse embryos. Nevertheless, our data demonstrate that a genetic cascade

440   comprising OC and Pou2f2 transcription factors ensures proper distribution of V2 cells

441   during spinal cord development. This program may not be restricted to V2 cells, as

442   diversification and distribution of dorsal INs and of motor neurons are also altered in the

443   absence of OC factors (Kabayiza et al., 2017, Roy et al., 2012) and as *Pou2f2* expression in

444   the OC mutant spinal cord is increased in multiple neuronal populations.

445 **Materials and methods**

446 **Ethics statement and mouse lines**

447 All experiments were strictly performed in accordance with the European Community

448 Council directive of 24 November 1986 (86-609/ECC) and the decree of 20 October 1987 (87-

449 848/EEC). Mice were raised in our animal facilities and treated according to the principles of

450 laboratory animal care, and experiments and mouse housing were approved by the Animal

451 Welfare Committee of Université catholique de Louvain (Permit Number: 2013/UCL/MD/11

452 and 2017/UCL/MD/008). The day of vaginal plug was considered to be embryonic day (e)

453 0.5. A minimum of three embryos of the same genotype was analyzed in each experiment.

454 The embryos were collected at e12.5 and e14.5. The *Hnf6;Oc2* and the *Pou2f2* mutant mice

455 were previously described (Clotman et al., 2005, Corcoran et al., 1993, Jacquemin et al.,

456 2000). In the $Hnf6^{-/-}Oc2^{-/-}$ embryos, expression of *Oc3* is completely downregulated in the

457 developing spinal cord (Kabayiza et al., 2017, Roy et al., 2012), enabling to study spinal cord

458 development in the absence of the 3 OC factors. The mice and the embryos were genotyped

459 by PCR (primer information available on request).

460

461 *In situ* **hybridization (ISH) and immunofluorescence labelings**

462 For ISH, the collected embryos were fixed in ice-cold 4% paraformaldehyde (PFA) in

463 phosphate buffered-saline (PBS) overnight at 4°C, washed thrice in PBS for 10 minutes,

464 incubated in PBS/30% sucrose solution overnight at 4°C, embedded and frozen in PBS/15%

465 sucrose/7.5% gelatin. Fourteen μm section were prepared and ISH was performed as

466 previously described (Beguin et al., 2013, Francius et al., 2016, Pelosi et al., 2014) with DIG-

467 conjugated Pou2f2 (NM_011138.1, nucleotides 604-1187) or Pou2f2 exon 5b

468 (XM_006539651.3, nucleotides 643-876) antisense RNA probes. Control and Onecut mutant

469 sections were placed adjacent on the same histology slides to minimize inter-slide variations

470 in ISH signals.

471 For immunofluorescence, collected embryos were fixed in 4% PFA/PBS for 25 or 35 minutes

472 according to their embryonic stage and processed as for ISH. Immunolabeling was

473 performed on 14 μm serial cryosections as previously described (Francius and Clotman,

474 2010). Primary antibodies against the following proteins were used: Chx10 (sheep; 1:500;

475 Exalpha Biologicals #X1179P), Foxp1 (goat; 1:1000; R&D Systems #AF4534), Gata3 (rat; 1:50;

476 Absea Biotechnology #111214D02), GFP (chick; 1:1000; Aves Lab #GFP-1020), HNF6 (guinea

477   pig; 1:2000; (Espana and Clotman, 2012b); or rabbit; 1:100; Santa Cruz #sc-13050; or sheep;

478   1:1000 R&D Systems #AF6277), cMaf (rabbit; 1:3000; kindly provided by H. Wende), MafA

479   (guinea pig; 1:500; kindly provide by T. Müller), OC2 (rat; 1:400; (Clotman et al., 2005); or

480   sheep; 1:500; R&D Systems #AF6294), OC3 (guinea pig; 1:6000; (Pierreux et al., 2004)),

481   Pou2f2 (rabbit; 1:2000; Abcam #ab178679), Shox2 (mouse; 1:500; Abcam #ab55740), Sox1

482   (goat; 1:500; Santa Cruz #sc-17318). Secondary antibodies donkey anti-guinea

483   pig/AlexaFluor 488, 594 or 647, anti-mouse/AlexaFluor 488, 594 or 647, anti-

484   rabbit/AlexaFluor 594 or 647, anti-goat/AlexaFluor 488, anti-rat/AlexaFluor 647, anti-

485   sheep/AlexaFluor 594 or 647, and goat anti-mouse IgG2A specific/AlexiaFluor 488,

486   purchased from ThermoFisher Scientific or Jackson Laboratories were used at dilution

487   1:2000 or 1:1000, respectively.

488

489   ***In ovo* electroporation**

490   *In ovo* electroporations were performed at stage HH14-16, as previously described (Roy et

491   al., 2012). The coding sequence of the S_Pou2f2.4 transcript was amplified by overlapping-

492   PCR using: forward 5' GCTCTGTCTGCCCAAGAGAAA 3' and reverse 5'

493   GTTGGGACAAGGTGAGCTGT 3' primers for the 5' sequence, forward 5'

494   CCACCATCACAGCCTACCAG 3' and reverse 5' ATTATCTCGAGCCAGCCTCCTTACCCTCTCT 3'

495   (designed to enable integration at the *Xho*I restriction site of the pCMV-MCS vector) primers

496   for the 3' sequence. This sequence was first subcloned in a pCR®II-Topo® vector (Life

497   Technologies, 45-0640) for sequencing then subcloned at the *Eco*RI (from the pCR®II-Topo®

498   vector) and *Xho*I restriction sites of a pCMV-MCS vector for the *in ovo* electroporation. The

499   pCMV-Pou2f2 (0.5 μg/μl) vector was co-electroporated with a pCMV-eGFP plasmid

500   (0.25μg/μl) to visualize electroporated cells. The embryos were collected 72 hours (HH27-

501   28) after electroporation, fixed in PBS/4%PFA for 45 minutes and processed for

502   immunofluorescence labelings as previously described (Francius and Clotman, 2010). To

503   minimize stage and experimental condition variations, the non-electroporated side of the

504   spinal cord was used as control for quantification and distribution analyses.

505

506   **Imaging and quantitative analyses**

507   Immunofluorescence and ISH images of cryosections were acquired on an EVOS FL Auto

508   Imaging System (Thermo Fisher Scientific) or a Confocal laser Scanning biological microscope

509   FV1000 Fluoview with the FV10-ASW 01.02 software (Olympus). The images were processed

510   with Adobe Photoshop CS5 software to match brightness and contrast with the observation.

511   Quantifications were performed by subtractive method (Francius and Clotman, 2010). For

512   each embryo ($n \geq 3$), one side of three to five sections at brachial, thoracic or lumbar level

513   were quantified using the count analysis tool of Adobe Photoshop CS5 software. Raw data

514   were exported from Adobe Photoshop CS5 software to Sigma Plotv12.3 software to perform

515   statistical analyses. The histograms were drawn with Microsoft Excel. Adequate statistical

516   tests (standard Student's *t*-tests or Mann-Whitney U tests) were applied depending on the

517   number of comparisons and on the variance in each group. Quantitative analyses were

518   considered significant at $p \leq 0.05$.

519   Quantitative analyzes of IN spatial distribution were performed as previously described

520   (Kabayiza et al., 2017). Statistical analyses of ventral IN distribution were performed using a

521   two-sample Hotelling's T2, which is a two-dimensional generalization of the Student's t test.

522   The analysis was implemented using the NCSS software package.

523

524   **Microarray analyses**

525   RNA was extracted from control or *Hnf6/Oc2* double-mutant spinal cords. The tissue was

526   manually dissociated in Tripur isolation reagent (Roche, 11 667 165 001). After dissociation,

527   chloroform (Merck Millipore, 1 02445 1000) was added to the sample, incubated at room

528   temperature for 10 minutes and centrifugated for 10 minutes at 4°C. The aqueous phase

529   was collected and the RNA was precipitated with isopropanol (VWR, 20880.310) and

530   centrifugated for 15 minutes at 4°C. The pellet was washed in ethanol (Biosolve, 06250502)

531   and centrifugated for 10 minutes at 4°C. The dried pellet was resuspended in RNAse free

532   water. The integrity of the RNA was assessed using an Agilent RNA 6000 Nano assay

533   procedure. For microarray analyzes, the RNA was converted in single-strand cDNA, labeled

534   using the GeneChip® WT PLUS Reagent Kit (Affymetrix) and hybridized on the GeneChip®

535   MoGene 2.0 ST array (Affymetrix, 90 2118) using Affymetrix devices: Genechip ® Fluidics

536   Station 450, Genechip® Hybridization oven 640, Affymetrix Genechip® scanner and the

537   Expression Consol software. The analyzes were performed using the R software. Microarray

538   data have been deposited in the GEO repository (accession number: GSE117871).

539

540

18

541 **Amplification of *Pou2f2* isoforms and sequencing**

542 Fragments of the different *Pou2f2* isoforms were amplified by RT-PCR from RNA of control B

543 lymphocytes or embryonic spinal cords purified as described above using the iScript™

544 Reverse transcriptase and the 5x iScript™ reaction mix (BioRad). *Pou2f2* sequences (Table 2)

545 were amplified using a GoTaq® Green master mix (Promega, M712) or a Q5® Hot Start High-

546 Fidelity DNA Polymerase (New England BioLabs® Inc, M0493S) (primer information available

547 on request). Sequencing of the spinal *Pou2f2* exons was outsourced to Genewiz.

548 Quantitative real-time PCR was performed on 1/100 of the retrotranscription reaction using

549 iTaq™ universal SYBR® Green Supermix (BioRad, 172-5124) on a CFX Connect™ Real-Time

550 System (BioRad) with the BioRad CFX Manage 3.1 software. Each reaction was performed in

551 duplicate and relative mRNA quantities were normalized to the housekeeping gene RPL32

552 (primer information available on request). Relative expression changes between conditions

553 were calculated using the $\Delta\Delta$Ct method. All changes are shown as fold changes.

554

Competing interests: the authors declare no competing interest

578 **References**

579 AMPATZIS, K., SONG, J., AUSBORN, J. & EL MANIRA, A. 2014. Separate microcircuit modules
580   of distinct v2a interneurons and motoneurons control the speed of locomotion.
581   *Neuron,* 83**,** 934-43.

582 AUDOUARD, E., SCHAKMAN, O., GINION, A., BERTRAND, L., GAILLY, P. & CLOTMAN, F. 2013.
583   The Onecut transcription factor HNF-6 contributes to proper reorganization of
584   Purkinje cells during postnatal cerebellum development. *Mol Cell Neurosci,* 56**,** 159-
585   68.

586 AUDOUARD, E., SCHAKMAN, O., RENE, F., HUETTL, R. E., HUBER, A. B., LOEFFLER, J. P.,
587   GAILLY, P. & CLOTMAN, F. 2012. The Onecut transcription factor HNF-6 regulates in
588   motor neurons the formation of the neuromuscular junctions. *PLoS One,* 7**,** e50509.

589 BARBER, M. & PIERANI, A. 2016. Tangential migration of glutamatergic neurons and cortical
590   patterning during development: Lessons from Cajal-Retzius cells. *Dev Neurobiol,* 76**,**
591   847-81.

592 BEAUDRY, J. B., PIERREUX, C. E., HAYHURST, G. P., PLUMB-RUDEWIEZ, N., WEISS, M. C.,
593   ROUSSEAU, G. G. & LEMAIGRE, F. P. 2006. Threshold levels of hepatocyte nuclear
594   factor 6 (HNF-6) acting in synergy with HNF-4 and PGC-1alpha are required for time-
595   specific gene expression during liver development. *Mol Cell Biol,* 26**,** 6037-46.

596 BEGUIN, S., CREPEL, V., ANIKSZTEJN, L., BECQ, H., PELOSI, B., PALLESI-POCACHARD, E.,
597   BOUAMRANE, L., PASQUALETTI, M., KITAMURA, K., CARDOSO, C. & REPRESA, A.
598   2013. An epilepsy-related ARX polyalanine expansion modifies glutamatergic neurons
599   excitability and morphology without affecting GABAergic neurons development.
600   *Cereb Cortex,* 23**,** 1484-94.

601 BIKOFF, J. B., GABITTO, M. I., RIVARD, A. F., DROBAC, E., MACHADO, T. A., MIRI, A.,
602   BRENNER-MORTON, S., FAMOJURE, E., DIAZ, C., ALVAREZ, F. J., MENTIS, G. Z. &
603   JESSELL, T. M. 2016. Spinal Inhibitory Interneuron Diversity Delineates Variant Motor
604   Microcircuits. *Cell,* 165**,** 207-19.

605 BLACKLAWS, J., DESKA-GAUTHIER, D., JONES, C. T., PETRACCA, Y. L., LIU, M., ZHANG, H.,
606   FAWCETT, J. P., GLOVER, J. C., LANUZA, G. M. & ZHANG, Y. 2015. Sim1 is required for
607   the migration and axonal projections of V3 interneurons in the developing mouse
608   spinal cord. *Dev Neurobiol,* 75**,** 1003-17.

609 BOIJE, H. & KULLANDER, K. 2018. Origin and circuitry of spinal locomotor interneurons
610   generating different speeds. *Curr Opin Neurobiol,* 53**,** 16-21.

611 BOROWSKA, J., JONES, C. T., DESKA-GAUTHIER, D. & ZHANG, Y. 2015. V3 interneuron
612   subpopulations in the mouse spinal cord undergo distinctive postnatal maturation
613   processes. *Neuroscience,* 295**,** 221-8.

614 BOROWSKA, J., JONES, C. T., ZHANG, H., BLACKLAWS, J., GOULDING, M. & ZHANG, Y. 2013.
615   Functional subpopulations of V3 interneurons in the mature mouse spinal cord. *J*
616   *Neurosci,* 33**,** 18553-65.

617 BRITZ, O., ZHANG, J., GROSSMANN, K. S., DYCK, J., KIM, J. C., DYMECKI, S., GOSGNACH, S. &
618   GOULDING, M. 2015. A genetically defined asymmetry underlies the inhibitory
619   control of flexor-extensor locomotor movements. *Elife,* 4.

620 CAMOS, S., GUBERN, C., SOBRADO, M., RODRIGUEZ, R., ROMERA, V. G., MORO, M. A.,
621   LIZASOAIN, I., SERENA, J., MALLOLAS, J. & CASTELLANOS, M. 2014. Oct-2
622   transcription factor binding activity and expression up-regulation in rat cerebral
623   ischaemia is associated with a diminution of neuronal damage in vitro.
624   *Neuromolecular Med,* 16**,** 332-49.

625 CATELA, C., SHIN, M. M. & DASEN, J. S. 2015. Assembly and function of spinal circuits for
626   motor control. *Annu Rev Cell Dev Biol,* 31**,** 669-98.

627 CLOTMAN, F., JACQUEMIN, P., PLUMB-RUDEWIEZ, N., PIERREUX, C. E., VAN DER SMISSEN,
628   P., DIETZ, H. C., COURTOY, P. J., ROUSSEAU, G. G. & LEMAIGRE, F. P. 2005. Control of
629   liver cell fate decision by a gradient of TGF beta signaling modulated by Onecut
630   transcription factors. *Genes Dev,* 19**,** 1849-54.

631 CLOVIS, Y. M., SEO, S. Y., KWON, J. S., RHEE, J. C., YEO, S., LEE, J. W., LEE, S. & LEE, S. K. 2016.
632   Chx10 Consolidates V2a Interneuron Identity through Two Distinct Gene Repression
633   Modes. *Cell Rep,* 16**,** 1642-52.

634 CORCORAN, L. M., KARVELAS, M., NOSSAL, G. J., YE, Z. S., JACKS, T. & BALTIMORE, D. 1993.
635   Oct-2, although not required for early B-cell development, is critical for later B-cell
636   maturation and for postnatal survival. *Genes Dev,* 7**,** 570-82.

637 CORCORAN, L. M., KOENTGEN, F., DIETRICH, W., VEALE, M. & HUMBERT, P. O. 2004. All
638   known in vivo functions of the Oct-2 transcription factor require the C-terminal
639   protein domain. *J Immunol,* 172**,** 2962-9.

640 CRONE, S. A., QUINLAN, K. A., ZAGORAIOU, L., DROHO, S., RESTREPO, C. E., LUNDFALD, L.,
641   ENDO, T., SETLAK, J., JESSELL, T. M., KIEHN, O. & SHARMA, K. 2008. Genetic ablation
642   of V2a ipsilateral interneurons disrupts left-right locomotor coordination in
643   mammalian spinal cord. *Neuron,* 60**,** 70-83.

644 DEL BARRIO, M. G., TAVEIRA-MARQUES, R., MUROYAMA, Y., YUK, D. I., LI, S., WINES-
645   SAMUELSON, M., SHEN, J., SMITH, H. K., XIANG, M., ROWITCH, D. & RICHARDSON, W.
646   D. 2007. A regulatory network involving Foxn4, Mash1 and delta-like 4/Notch1
647   generates V2a and V2b spinal interneurons from a common progenitor pool.
648   *Development,* 134**,** 3427-36.

649 DOUGHERTY, K. J. & KIEHN, O. 2010. Firing and cellular properties of V2a interneurons in the
650   rodent spinal cord. *J Neurosci,* 30**,** 24-37.

651 DOUGHERTY, K. J., ZAGORAIOU, L., SATOH, D., ROZANI, I., DOOBAR, S., ARBER, S., JESSELL, T.
652   M. & KIEHN, O. 2013. Locomotor rhythm generation linked to the output of spinal
653   shox2 excitatory interneurons. *Neuron,* 80**,** 920-33.

654 ESPANA, A. & CLOTMAN, F. 2012a. Onecut factors control development of the Locus
655   Coeruleus and of the mesencephalic trigeminal nucleus. *Mol Cell Neurosci,* 50**,** 93-
656   102.

657 ESPANA, A. & CLOTMAN, F. 2012b. Onecut transcription factors are required for the second
658   phase of development of the A13 dopaminergic nucleus in the mouse. *J Comp
659   Neurol,* 520**,** 1424-41.

660 FRANCIUS, C. & CLOTMAN, F. 2010. Dynamic expression of the Onecut transcription factors
661   HNF-6, OC-2 and OC-3 during spinal motor neuron development. *Neuroscience,* 165**,**
662   116-29.

663 FRANCIUS, C. & CLOTMAN, F. 2014. Generating spinal motor neuron diversity: a long quest
664   for neuronal identity. *Cell Mol Life Sci,* 71**,** 813-29.

665 FRANCIUS, C., HARRIS, A., RUCCHIN, V., HENDRICKS, T. J., STAM, F. J., BARBER, M., KUREK,
666   D., GROSVELD, F. G., PIERANI, A., GOULDING, M. & CLOTMAN, F. 2013. Identification
667   of multiple subsets of ventral interneurons and differential distribution along the
668   rostrocaudal axis of the developing spinal cord. *PLoS One,* 8**,** e70325.

669 FRANCIUS, C., HIDALGO-FIGUEROA, M., DEBRULLE, S., PELOSI, B., RUCCHIN, V.,
670   RONELLENFITCH, K., PANAYIOTOU, E., MAKRIDES, N., MISRA, K., HARRIS, A.,
671   HASSANI, H., SCHAKMAN, O., PARRAS, C., XIANG, M., MALAS, S., CHOW, R. L. &

672   CLOTMAN, F. 2016. Vsx1 Transiently Defines an Early Intermediate V2 Interneuron
673   Precursor Compartment in the Mouse Developing Spinal Cord. *Front Mol Neurosci,* 9**,**
674   145.
675 GOETZ, C., PIVETTA, C. & ARBER, S. 2015. Distinct limb and trunk premotor circuits establish
676   laterality in the spinal cord. *Neuron,* 85**,** 131-144.
677 GOSGNACH, S., BIKOFF, J. B., DOUGHERTY, K. J., EL MANIRA, A., LANUZA, G. M. & ZHANG, Y.
678   2017. Delineating the Diversity of Spinal Interneurons in Locomotor Circuits. *J*
679   *Neurosci,* 37**,** 10835-10841.
680 GROSSMANN, K. S., GIRAUDIN, A., BRITZ, O., ZHANG, J. & GOULDING, M. 2010. Genetic
681   dissection of rhythmic motor networks in mice. *Prog Brain Res,* 187**,** 19-37.
682 GUO, J. & ANTON, E. S. 2014. Decision making during interneuron migration in the
683   developing cerebral cortex. *Trends Cell Biol,* 24**,** 342-51.
684 HATZOPOULOS, A. K., STOYKOVA, A. S., ERSELIUS, J. R., GOULDING, M., NEUMAN, T. &
685   GRUSS, P. 1990. Structure and expression of the mouse Oct2a and Oct2b, two
686   differentially spliced products of the same gene. *Development,* 109**,** 349-62.
687 HAYASHI, M., HINCKLEY, C. A., DRISCOLL, S. P., MOORE, N. J., LEVINE, A. J., HILDE, K. L.,
688   SHARMA, K. & PFAFF, S. L. 2018. Graded Arrays of Spinal and Supraspinal V2a
689   Interneuron Subtypes Underlie Forelimb and Hindlimb Motor Control. *Neuron,* 97**,**
690   869-884 e5.
691 HILDE, K. L., LEVINE, A. J., HINCKLEY, C. A., HAYASHI, M., MONTGOMERY, J. M., GULLO, M.,
692   DRISCOLL, S. P., GROSSCHEDL, R., KOHWI, Y., KOHWI-SHIGEMATSU, T. & PFAFF, S. L.
693   2016. Satb2 Is Required for the Development of a Spinal Exteroceptive Microcircuit
694   that Modulates Limb Position. *Neuron,* 91**,** 763-776.
695 HODSON, D. J., SHAFFER, A. L., XIAO, W., WRIGHT, G. W., SCHMITZ, R., PHELAN, J. D., YANG,
696   Y., WEBSTER, D. E., RUI, L., KOHLHAMMER, H., NAKAGAWA, M., WALDMANN, T. A. &
697   STAUDT, L. M. 2016. Regulation of normal B-cell differentiation and malignant B-cell
698   survival by OCT2. *Proc Natl Acad Sci U S A,* 113**,** E2039-46.
699 JACQUEMIN, P., DURVIAUX, S. M., JENSEN, J., GODFRAIND, C., GRADWOHL, G., GUILLEMOT,
700   F., MADSEN, O. D., CARMELIET, P., DEWERCHIN, M., COLLEN, D., ROUSSEAU, G. G. &
701   LEMAIGRE, F. P. 2000. Transcription factor hepatocyte nuclear factor 6 regulates
702   pancreatic endocrine cell differentiation and controls expression of the proendocrine
703   gene ngn3. *Mol Cell Biol,* 20**,** 4445-54.
704 JACQUEMIN, P., LANNOY, V. J., ROUSSEAU, G. G. & LEMAIGRE, F. P. 1999. OC-2, a novel
705   mammalian member of the ONECUT class of homeodomain transcription factors
706   whose function in liver partially overlaps with that of hepatocyte nuclear factor-6. *J*
707   *Biol Chem,* 274**,** 2665-71.
708 JACQUEMIN, P., LEMAIGRE, F. P. & ROUSSEAU, G. G. 2003a. The Onecut transcription factor
709   HNF-6 (OC-1) is required for timely specification of the pancreas and acts upstream
710   of Pdx-1 in the specification cascade. *Dev Biol,* 258**,** 105-16.
711 JACQUEMIN, P., PIERREUX, C. E., FIERENS, S., VAN EYLL, J. M., LEMAIGRE, F. P. & ROUSSEAU,
712   G. G. 2003b. Cloning and embryonic expression pattern of the mouse Onecut
713   transcription factor OC-2. *Gene Expr Patterns,* 3**,** 639-44.
714 JOSHI, K., LEE, S., LEE, B., LEE, J. W. & LEE, S. K. 2009. LMO4 controls the balance between
715   excitatory and inhibitory spinal V2 interneurons. *Neuron,* 61**,** 839-51.
716 KABAYIZA, K. U., MASGUTOVA, G., HARRIS, A., RUCCHIN, V., JACOB, B. & CLOTMAN, F. 2017.
717   The Onecut Transcription Factors Regulate Differentiation and Distribution of Dorsal
718   Interneurons during Spinal Cord Development. *Front Mol Neurosci,* 10**,** 157.

719 KONIG, H., PFISTERER, P., CORCORAN, L. M. & WIRTH, T. 1995. Identification of CD36 as the
720   first gene dependent on the B-cell differentiation factor Oct-2. *Genes Dev,* 9, 1598-
721   607.
722 LAI, H. C., SEAL, R. P. & JOHNSON, J. E. 2016. Making sense out of spinal cord somatosensory
723   development. *Development,* 143, 3434-3448.
724 LANDRY, C., CLOTMAN, F., HIOKI, T., ODA, H., PICARD, J. J., LEMAIGRE, F. P. & ROUSSEAU, G.
725   G. 1997. HNF-6 is expressed in endoderm derivatives and nervous system of the
726   mouse embryo and participates to the cross-regulatory network of liver-enriched
727   transcription factors. *Dev Biol,* 192, 247-57.
728 LANNOY, V. J., RODOLOSSE, A., PIERREUX, C. E., ROUSSEAU, G. G. & LEMAIGRE, F. P. 2000.
729   Transcriptional stimulation by hepatocyte nuclear factor-6. Target-specific
730   recruitment of either CREB-binding protein (CBP) or p300/CBP-associated factor
731   (p/CAF). *J Biol Chem,* 275, 22098-103.
732 LATCHMAN, D. S. 1996. The Oct-2 transcription factor. *Int J Biochem Cell Biol,* 28, 1081-3.
733 LEE, S., LEE, B., JOSHI, K., PFAFF, S. L., LEE, J. W. & LEE, S. K. 2008. A regulatory network to
734   segregate the identity of neuronal subtypes. *Dev Cell,* 14, 877-89.
735 LEMAIGRE, F. P., DURVIAUX, S. M., TRUONG, O., LANNOY, V. J., HSUAN, J. J. & ROUSSEAU, G.
736   G. 1996. Hepatocyte nuclear factor 6, a transcription factor that contains a novel type
737   of homeodomain and a single cut domain. *Proc Natl Acad Sci U S A,* 93, 9460-4.
738 LILLYCROP, K. A. & LATCHMAN, D. S. 1992. Alternative splicing of the Oct-2 transcription
739   factor RNA is differentially regulated in neuronal cells and B cells and results in
740   protein isoforms with opposite effects on the activity of octamer/TAATGARAT-
741   containing promoters. *J Biol Chem,* 267, 24960-5.
742 LIU, Y. Z., LILLYCROP, K. A. & LATCHMAN, D. S. 1995. Regulated splicing of the Oct-2
743   transcription factor RNA in neuronal cells. *Neurosci Lett,* 183, 8-12.
744 LU, D. C., NIU, T. & ALAYNICK, W. A. 2015. Molecular and cellular development of spinal cord
745   locomotor circuitry. *Front Mol Neurosci,* 8, 25.
746 MISRA, K., LUO, H., LI, S., MATISE, M. & XIANG, M. 2014. Asymmetric activation of Dll4-
747   Notch signaling by Foxn4 and proneural factors activates BMP/TGFbeta signaling to
748   specify V2b interneurons in the spinal cord. *Development,* 141, 187-98.
749 PANAYI, H., PANAYIOTOU, E., ORFORD, M., GENETHLIOU, N., MEAN, R., LAPATHITIS, G., LI, S.,
750   XIANG, M., KESSARIS, N., RICHARDSON, W. D. & MALAS, S. 2010. Sox1 is required for
751   the specification of a novel p2-derived interneuron subtype in the mouse ventral
752   spinal cord. *J Neurosci,* 30, 12274-80.
753 PELOSI, B., MIGLIARINI, S., PACINI, G., PRATELLI, M. & PASQUALETTI, M. 2014. Generation of
754   Pet1210-Cre transgenic mouse line reveals non-serotonergic expression domains of
755   Pet1 both in CNS and periphery. *PLoS One,* 9, e104318.
756 PENG, C. Y., YAJIMA, H., BURNS, C. E., ZON, L. I., SISODIA, S. S., PFAFF, S. L. & SHARMA, K.
757   2007. Notch and MAML signaling drives Scl-dependent interneuron diversity in the
758   spinal cord. *Neuron,* 53, 813-27.
759 PIERREUX, C. E., VANHORENBEECK, V., JACQUEMIN, P., LEMAIGRE, F. P. & ROUSSEAU, G. G.
760   2004. The transcription factor hepatocyte nuclear factor-6/Onecut-1 controls the
761   expression of its paralog Onecut-3 in developing mouse endoderm. *J Biol Chem,* 279,
762   51298-304.
763 ROY, A., FRANCIUS, C., ROUSSO, D. L., SEUNTJENS, E., DEBRUYN, J., LUXENHOFER, G., HUBER,
764   A. B., HUYLEBROECK, D., NOVITCH, B. G. & CLOTMAN, F. 2012. Onecut transcription

765   factors act upstream of Isl1 to regulate spinal motoneuron diversification.
766   *Development,* 139**,** 3109-19.

767 STAM, F. J., HENDRICKS, T. J., ZHANG, J., GEIMAN, E. J., FRANCIUS, C., LABOSKY, P. A.,
768   CLOTMAN, F. & GOULDING, M. 2012. Renshaw cell interneuron specialization is
769   controlled by a temporally restricted transcription factor program. *Development,*
770   139**,** 179-90.

771 STOYKOVA, A. S., STERRER, S., ERSELIUS, J. R., HATZOPOULOS, A. K. & GRUSS, P. 1992. Mini-
772   Oct and Oct-2c: two novel, functionally diverse murine Oct-2 gene products are
773   differentially expressed in the CNS. *Neuron,* 8**,** 541-58.

774 SURMELI, G., AKAY, T., IPPOLITO, G. C., TUCKER, P. W. & JESSELL, T. M. 2011. Patterns of
775   spinal sensory-motor connectivity prescribed by a dorsoventral positional template.
776   *Cell,* 147**,** 653-65.

777 SWEENEY, L. B., BIKOFF, J. B., GABITTO, M. I., BRENNER-MORTON, S., BAEK, M., YANG, J. H.,
778   TABAK, E. G., DASEN, J. S., KINTNER, C. R. & JESSELL, T. M. 2018. Origin and
779   Segmental Diversity of Spinal Inhibitory Interneurons. *Neuron,* 97**,** 341-355 e3.

780 TALPALAR, A. E., BOUVIER, J., BORGIUS, L., FORTIN, G., PIERANI, A. & KIEHN, O. 2013. Dual-
781   mode operation of neuronal networks involved in left-right alternation. *Nature,* 500**,**
782   85-8.

783 THALER, J. P., LEE, S. K., JURATA, L. W., GILL, G. N. & PFAFF, S. L. 2002. LIM factor Lhx3
784   contributes to the specification of motor neuron and interneuron identity through
785   cell-type-specific protein-protein interactions. *Cell,* 110**,** 237-49.

786 THEODOROU, E., DALEMBERT, G., HEFFELFINGER, C., WHITE, E., WEISSMAN, S., CORCORAN,
787   L. & SNYDER, M. 2009. A high throughput embryonic stem cell screen identifies Oct-2
788   as a bifunctional regulator of neuronal differentiation. *Genes Dev,* 23**,** 575-88.

789 TRIPODI, M., STEPIEN, A. E. & ARBER, S. 2011. Motor antagonism exposed by spatial
790   segregation and timing of neurogenesis. *Nature,* 479**,** 61-6.

791 VANHORENBEECK, V., JACQUEMIN, P., LEMAIGRE, F. P. & ROUSSEAU, G. G. 2002. OC-3, a
792   novel mammalian member of the ONECUT class of transcription factors. *Biochem*
793   *Biophys Res Commun,* 292**,** 848-54.

794 WIRTH, T., PRIESS, A., ANNWEILER, A., ZWILLING, S. & OELER, B. 1991. Multiple Oct2
795   isoforms are generated by alternative splicing. *Nucleic Acids Res,* 19**,** 43-51.

796 ZISKIND-CONHAIM, L. & HOCHMAN, S. 2017. Diversity of molecularly defined spinal
797   interneurons engaged in mammalian locomotor pattern generation. *J Neurophysiol,*
798   118**,** 2956-2974.

799

800

801

802

803 **Figure legends**

804

805 **Figure 1. OC factors are present in multiple subsets of V2 interneurons. (A-I")**

806 Immunolabelings for OC, the V2a generic marker Chx10 and markers of V2a subpopulations

807 (Francius et al., 2013) on transverse spinal cord sections (brachial or thoracic levels) of e12.5

808 wild-type mouse embryos. In each figure, the right ventral quadrant of the spinal cord is

809 shown. Only HNF-6 is detected in Shox2+ V2a cells (arrow in A-C''), whereas the 3 OC are

810 present in the MafA+ and in the cMaf+ V2a subsets (arrows in D-I"). **(J-L")** Immunolabelings

811 for OC, the V2b generic marker Gata3 and MafA. The 3 OC proteins are detected in MafA+

812 V2b interneurons (arrows). **(M-O")** Immunolabelings for OC and the V2c marker Sox1

813 demonstrate that OC factors are present in a majority of V2c interneurons (arrows). Sox1 in

814 the ventricular zone labels neural progenitors. Scale bar = 50 µm.

815

816 **Figure 2. OC factors regulate the diversification of the V2 interneurons.** Immunolabelings

817 on transverse spinal cord sections (brachial or thoracic levels) of control or $Hnf6^{-/-};Oc2^{-/-}$

818 double-mutant embryos. At e12.5 **(A-C)** and e14.5 **(D)**, the production of the V2a Chx10+

819 interneurons is not altered in the absence of OC factors. Similarly, the number of

820 Shox2+ V2a is affected neither at e12.5 **(E-G)** nor at e14.5 **(H)**. In contrast, quantitative

821 analysis of control or $Hnf6^{-/-};Oc2^{-/-}$ littermates at e12.5 **(I-K)** and at e14.5 **(L)** shows reduction

822 in MafA+ V2a interneurons in double mutants as compared to control embryos. Similarly,

823 the number of cMaf+ V2a interneurons is significantly reduced at e12.5 (**M-O**) and e14.5 (**P**)

824 in the absence of OC factors. At e12.5 **(Q-S)** and e14.5 **(T)**, the production of the V2b

825 interneurons is not affected in $Hnf6^{-/-};Oc2^{-/-}$ embryos. The generation of the MafA+ V2b

826 interneurons is also unchanged at e12.5 **(U-W)** or e14.5 **(X)**. At e12.5 **(Y-AA)**, the number of

827 V2c interneurons is dramatically reduced in the absence of OC factors (Sox1 in the

828 ventricular zone labels neural progenitors). However, this is no longer the case at e14.5 **(BB)**.

829 Mean values ± SEM. * p≤0.05 ; ** p≤0.01 ; *** p≤0.001. Scale bar = 50 µm.

830

831 **Figure 3. OC factors regulate the distribution of V2a interneurons.** Distribution of V2a

832 interneurons on the transverse plane of the spinal cord in control or $Hnf6^{-/-};Oc2^{-/-}$ double-

833 mutant embryos at brachial, thoracic or lumbar level (only the right hemisection is shown).

834 Two-dimension distribution graphs (left) show integration of cell distribution from multiple

835   sections of multiple embryos of each genotype. One-dimension graphs (right) compare

836   density distribution in control (blue) and in double-mutant embryos (red) on the dorso-

837   ventral (upper) or the medio-lateral (lower) axis of the spinal cord (see Materials and

838   methods for details). **(A-C)** At e12.5 in control embryos, V2a interneurons distribute in 2

839   connected clusters, a major central group and a minor medial group, at each level of the

840   spinal cord. **(D-L)** In mutant embryos, the relative cell distribution between the 2 clusters

841   seems altered, with relatively less central cells at brachial level and less medial cells at

842   lumbar levels (n=3, p≤0.001 at brachial and lumbar levels; p=0.17 at thoracic level). **(M-X)**

843   Altered V2a distribution on the medio-lateral axis is confirmed at e14.5. **(M-O, S-X)** In

844   control embryos, the 2 V2a groups coalesce in a more evenly-distributed population that

845   occupied ~70% of the medio-lateral axis. **(P-X)** In mutant embryos, V2a interneurons remain

846   segregated into 2 distinct, although connected, clusters with a majority of cells in medial

847   position (n=3, p≤0.001).

848

849   **Figure 4. OC factors regulate the distribution of V2b interneurons. (A-C)** At e12.5 in control

850   embryos, V2b cells are distributed in a major central (brachial level) or lateral (thoracic and

851   lumbar levels) cluster with minor subsets located more medially (arrows) or ventrally

852   (arrowheads). **(D-L)** In OC mutant embryos at e12.5, the major population remains more

853   compact, more centrally located and slightly more ventral. In addition, the ventral V2b

854   subset is significantly depleted (asterisks; n=3, p≤0.001 at brachial and thoracic levels;

855   p=0.31 at brachial level). **(M-X)** Consistently, at e14.5, V2b interneurons in the central

856   cluster are more compact in the absence of OC factors at thoracic level, and a small

857   contingent of V2b migrating towards the medio-dorsal spinal cord in control embryos

858   (arrowheads) is missing in OC mutant littermates (n=3, p≤0.001 at thoracic level; p=0.31 and

859   0.80 at thoracic and lumbar levels, respectively).

860

861   **Figure 5. OC factors control expression of spinal cord-specific isoforms of *Pou2f2*. (A)** The

862   different Pou2f2 isoforms present in the B cells (B_Pou2f2) are characterized by invariant

863   exons (dark grey) and alternative exons 4, 5, 8, 14 or 16 (light grey). They contain a POU-

864   specific domain (light green) encoded by exons 9 and 10 and a POU-type homeodomain

865   (dark green) encoded by exons 11 and 12. The 4 spinal Pou2f2 isoforms (S_Pou2f2.1 to

866   S_Pou2f2.4) (identified in the spinal cord) are characterized by a distinct exon 1 (E1X in light

orange), an additional exon E5b (dark orange) and alternative exons E1b and 4 (medium orange and light grey, respectively). The presence of E1b disrupts the reading frame and imposes the use of the ATG located in E2a, whereas the absence of E1b leaves open the use of the ATG located in E1X. The regions corresponding to the generic or to the E5b *in situ* hybridization probes are indicated. **(B-E)** Quantification of spinal Pou2f2 or B-cell isoforms by RT-qPCR. **(B)** In control spinal cords, spinal Pou2f2 isoforms are >30-fold more abundant than B-cell isoforms. **(C)** B cell Pou2f2 isoforms barely trend to increase in the absence of OC factors. **(D)** In contrast, spinal Pou2f2 isoforms are 2.6-fold overexpressed in *Hnf6$^{-/-}$;Oc2$^{-/-}$* spinal cords. **(E)** In double mutant spinal cords, spinal Pou2f2 isoforms are >60-fold more abundant than B-cell isoforms. **(F-I)** *In situ* hybridization labelings on transverse sections (brachial level) of control or *Hnf6$^{-/-}$;Oc2$^{-/-}$* spinal cords at e11.5 with **(F-G)** a generic *Pou2f2* probe complementary to spinal and to B-cell isoforms **(A)** or **(H-I)** a spinal isoform-specific probe corresponding only to exon E5b **(A)**. **(F, H)** In control embryos, *Pou2f2* is strongly expressed in ventral and in dorsal interneuron populations, and more weakly in the ventral motor neuron area. **(G, I)** In OC mutant embryos, *Pou2f2* is upregulated in interneuron populations and its expression is expanded in ventral populations (arrowheads) and in the motor neurons (arrows). * p≤0.05 ; ** p≤0.01. Scale bars = 50 μm.

Figure 6. The Pou2f2+ V2a interneurons are mislocated in the absence of OC factors. (A-F) Immunolabelings and quantification of Pou2f2+ V2a interneurons in control or *Hnf6$^{-/-}$;Oc2$^{-/-}$* mutant embryos. At e12.5 **(A-B)** and e14.5 **(C-D)**, Pou2f2 is detected in V2a Chx10^{+} interneurons, and the number of Pou2f2-containing Chx10+ cells trends to increase but is not significantly different in the absence of OC factors **(E-F)**. **(G-DD)** Distribution of Pou2f2+ V2a interneurons on the transverse plane of the spinal cord in control or *Hnf6$^{-/-}$;Oc2$^{-/-}$* double-mutant embryos. One-dimension graphs (lower) show density distribution on the dorso-ventral (left) or the medio-lateral (right) axis of the spinal cord. **(G-R)** At e12.5, cells in the central clusters are slightly reduced at brachial and at thoracic levels in the absence of OC factors (n=3, p≤0.001 at brachial and thoracic levels; p=0.41 at lumbar level). **(S-DD)** At e14.5, a vast majority of V2a containing Pou2f2 settles in a more medial position in *Hnf6$^{-/-}$;Oc2$^{-/-}$* spinal cords (n=3, p≤0.001). Mean values ± SEM. Scale bar = 50 μm.

28

898 **Figure 7. The Pou2f2+ V2b interneurons are mislocated in the absence of OC factors. (A-F)**

899 Immunolabelings and quantification of Pou2f2+ V2b interneurons in control or *Hnf6⁻/⁻;Oc2⁻/⁻*

900 mutant embryos. At e12.5 **(A-B)** and e14.5 **(C-D)**, Pou2f2 is present in V2b Gata3+

901 interneurons, but the number of Pou2f2+ V2b cells was not significantly increased in the

902 absence of OC factors **(E-F)**. **(G-DD)** Distribution of Pou2f2+ V2b interneurons on the

903 transverse plane of the spinal cord in control or *Hnf6⁻/⁻;Oc2⁻/⁻* double-mutant embryos. One-

904 dimension graphs (lower) show density distribution on the dorso-ventral (left) or the medio-

905 lateral (right) axis of the spinal cord. **(G-R)** At e12.5, Pou2f2-containing V2b are more central

906 and slightly more ventral in the absence of OC factors (n=3, p≤0.001). **(S-DD)** At e14.5, this

907 subset of V2b interneurons is more clustered on the medio-lateral axis in *Hnf6⁻/⁻;Oc2⁻/⁻* spinal

908 cords (n=3, p≤0.001). Mean values ± SEM. Scale bar = 50 μm.

909

910 **Figure 8. V2 interneuron distribution is altered after misexpression of *Pou2f2.***

911 Overexpression of *Pou2f2* in chick embryonic spinal cord after electroporation at HH14-16

912 and immunolabelings 72 hours after electroporation. **(A-F)** At HH27-28, *Pou2f2*

913 overexpression does not impact the number of V2a **(E)** or V2b **(F)** interneurons. In contrast,

914 it alters V2 distribution. **(G-J)** In control spinal cord, V2a interneurons are distributed in two

915 closely connected clusters on the medio-lateral axis of the neuroepithelium. In

916 electroporated spinal cord, lateral migration is increased and a majority of V2a interneurons

917 are clustered in a single central group with ectopic lateral extensions (arrows; n=3, p≤0.001).

918 **(K-N)** In control spinal cord, V2b are distributed in two groups along the medio-lateral axis

919 with a majority of cells in the lateral cluster. In electroporated spinal cord, the V2b

920 interneurons are equally distributed between these 2 clusters (n=3, p≤0.001). Mean values ±

921 SEM. Scale bar = 50 μm.

922

923 **Figure 9. Pou2f2 regulate the distribution of V2a interneurons. (A-C)** Immunolabelings and

924 quantification of V2a interneurons in control or *Pou2f2⁻/⁻* mutant embryos. At e12.5, the

925 production of the Chx10+ V2a interneurons is not altered in absence of Pou2f2. **(D-O)**

926 Distribution of V2a and Shox2+ V2a interneurons on the transverse plane of the spinal cord

927 in control or *Pou2f2⁻/⁻* mutant embryos. One-dimension graphs (right) show density

928 distribution on the dorso-ventral (upper) or the medio-lateral (lower) axis of the spinal cord.

929 V2a distribution is affected in *Pou2f2⁻/⁻* mutants. As compared to the two V2a clusters

930   observed in control embryos, Chx10+ cells are relatively more abundant in the medial cluster

931   in *Pou2f2⁻ᐟ⁻* mutant embryos (n=3, p≤0.001). Mean values ± SEM. Scale bar = 50 μm.

932

933   **Figure 10. Pou2f2 regulate the distribution of V2b interneurons. (A-C)** Immunolabelings and

934   quantification of V2b interneurons in control or *Pou2f2⁻ᐟ⁻* mutant embryos. At e12.5, the

935   production of the Gata3+ V2b interneurons is not affected by the absence of Pou2f2. **(D-O)**

936   Distribution of V2b interneurons on the transverse plane of the spinal cord in control or

937   *Pou2f2⁻ᐟ⁻* mutant embryos. One-dimension graphs (right) show density distribution on the

938   dorso-ventral (upper) or the medio-lateral (lower) axis of the spinal cord. The distribution of

939   V2b cells is altered in *Pou2f2⁻ᐟ⁻* mutants, as V2b interneurons remained more medial at

940   thoracic level and segregated more extensively on the medio-lateral axis at lumbar level

941   (n=3, p≤0.001). Mean values ± SEM. Scale bar = 50 μm.

942

943

944   **Supplementary figure legends**

945

946   **Supplementary Figure S1. OC factors regulate the diversification of the V2 interneurons.**

947   **(A-H'')** Immunolabelings of the V2a generic marker Chx10 and markers of V2a

948   subpopulations on transverse spinal cord sections (brachial or thoracic levels) control or

949   *Hnf6⁻ᐟ⁻;Oc2⁻ᐟ⁻* mutant embryos at e14.5. Quantifications are shown in Fig 1. V2a **(A-B),** Shox2+

950   V2a (arrows) and V2d interneurons (**C- D''**, arrowheads) are present in both control and

951   double mutant embryos. **(E-E'')** MafA is present in a V2a supbopulation in control embryos

952   (arrows), **(F-F'')** but is not detected in Chx10+ cells in the absence of OC factors. **(G-G'')**

953   Similarly**,** cMaf is present in a subpopulation of V2a interneurons in control embryos

954   (arrows), **(H-H'')** which is not the case in *Hnf6⁻ᐟ⁻;Oc2⁻ᐟ⁻* embryos. **(I-L'')** Immunolabelings of

955   the V2b generic marker Gata3 and the marker of V2b subpopulation, MafA. V2b **(I-J'')** and

956   MafA+ V2b (**K-L''**, arrows) interneurons are present in control and in *Hnf6⁻ᐟ⁻;Oc2⁻ᐟ⁻* embryos.

957   **(M-N)** The number of V2c interneurons is unchanged is similarly detected in *Hnf6⁻ᐟ⁻;Oc2⁻ᐟ⁻*

958   embryos as compared to control embryos (delineated cells). Sox1 in the ventricular zone

959   labels neural progenitors. Scale bar = 50 μm.

960

Supplementary Figure S2. Pou2f2 RT-PCR experiments and sequencing of exon 1b and exon 5b of the spinal Pou2f2 isoforms. Composite assembly of electrophoresis images of RT-PCR amplification products for *Pou2f2* isoform sequences on embryonic spinal cord or B-cell RNA samples. Water was used as a negative control (Ctl-). **(A)** Amplifications from exon 1 (E1) to E6 on embryonic spinal cord RNA samples (asterisk) fail to amplify the RNA isoforms detected in B cell samples. In contrast, amplifications from E7 to E9, from E10 to E12 and from E13 to E17 show at least one similar amplicon in spinal cord samples and in B cell samples. **(B)** Amplification from E1 (other forward primer) to E7 also fails to amplify *Pou2f2* spinal cord isoforms. In contrast, amplifications from E2, 3, 4 and 5 to E7 produce systematically longer amplicons in spinal cord samples (arrowheads) as compared to B cell samples. The E6 to E7 amplification is similar in both samples. **(C)** Amplifications from E1X (present in the X6 sequence) to E3 do not produce amplicon in B-cell samples (asterisk). Amplifications from E1X to E3 or to E5b on spinal cord samples systematically produce 2 amplicons (arrowheads). Amplifications of the E5b exon sequence, from E3 to E5b and from E5b to E7 produce expected amplicons in spinal cord samples. **(D)** Comparison of exon 1b and exon 5b sequences in the predicted X6 sequence and the sequenced embryonic spinal cord *Pou2f2* isoforms. Sequences of E1X, E2a and E5b exons align (100% identity) with the predicted X6 sequence. Sequence of the additional alterative exon 1b is shown. SD = Size standard, E = Exon, SC = Embryonic spinal cord, B = B lymphocytes.

Supplementary Figure S3. The number of Pou2f2+Shox2+ V2a interneurons is normal in *Hnf6$^{-/-}$;Oc2$^{-/-}$* mutant embryos. Immunolabelings on transverse spinal cord sections (brachial or thoracic levels) of control or *Hnf6$^{-/-}$;Oc2$^{-/-}$* mutant embryos. At e12.5 **(A-C)** and at e14.5 **(D-F)**, the number of V2a containing Shox2 and Pou2f2 is unchanged in the absence of OC factors. Mean values ± SEM. Scale bar = 50 μm.

Supplementary Figure S4. Efficacy of pCMV-eGFP and pCMV-Pou2f2 co-electroporation in the chicken embryonic spinal cord. (A-C) eGFP (green, **B**) and Pou2f2 (red, **C**) are present in a vast majority of cells along the dorso-ventral axis of the spinal cord. Scale bar = 50 μm.

Supplementary Figure S5. The number of MafA+ or cMaf+ V2a interneurons is normal in *Pou2f2$^{-/-}$* mutant spinal cords. Immunolabelings on transverse spinal cord sections (brachial

993   or thoracic levels) of control or *Pou2f2-/-* mutant embryos at e12.5. **(A-F)** Absence of Pou2f2

994   does not impact on the number of Shox2+ **(A-C),** cMaf+ **(D-F)** or MafA+ **(G-I)** V2a

995   interneurons. Mean values ± SEM. Scale bar = 50 μm.

996

997   **Supplementary Figure S6. The number of MafA-positive V2b interneurons or of the V2c**

998   **interneurons is normal in *Pou2f2-/-* mutant spinal cords.** Immunolabelings on transverse

999   spinal cord sections (brachial or thoracic levels) of control or *Pou2f2-/-* mutant embryos at

1000   e12.5. **(A-B, E)** The number of MafA+ V2b interneurons is not significantly altered in the

1001   absence of Pou2f2. **(C-D, F)** Similarly, the production of V2c interneurons is not affected in

1002   *Pou2f2* mutants. Mean values ± SEM. Scale bar = 50 μm.

1003

Table 1. OC factors are present in specific populations and subpopulations of V2 interneurons.

V2 – e12.5				
Populations	**Subpopulations**	**HNF-6**	**OC-2**	**OC-3**
V2a – Chx10		+	+	+
	Shox2	+	-	-
	MafA	+	+	+
	cMaf	+	+	+
	Bhlhb5	-	-	-
	Prdm8	-	-	-
V2b – Gata3		+	+	+
	MafA	+	+	+
	MafB	-	-	-
	Bhlhb5	-	-	-
	Prdm8	-	-	-
V2c – Sox1		+	+	+
V2d – Shox2		-	-	-

The V2 populations, including V2a, V2b, V2c and V2d, are subdivided in smaller subpopulations characterized by differential expression of transcription factors (Francius et al. 2013). OC factors are detected in specific populations and subpopulations of V2 interneurons.

Table 2. Pou2f2 isoforms in the developing spinal cord are different from B-cell isoforms.

Amplification	Expected sizes	B cells	Control spinal cord
E1 → E6	272 bp 390 bp 456 bp	272 bp 390 bp 456 bp	No amplification
E7 → E9	174 bp 222 bp	174 bp 222 bp	174 bp
E10 → E12	452 bp	452 bp	452 bp
E13 → E17	160 bp 296 bp 370 bp	160 bp 296 bp 370 bp	370 bp
E1 → E7	348bp 466 bp 532 bp	466 bp 532 bp	No amplification
E2 → E7	284 bp 402 bp 468 bp	402 bp 468 bp	~ 680 bp ~ 750 bp
E3 → E6	154 bp 272 bp 378 bp	154 bp 272 bp 378 bp	272 bp 378 bp ~ 550 bp ~ 650 bp
E4 → E7	340 bp	340 bp	~ 600 bp
E5 → E7	201 bp	201 bp	201 bp ~ 480 bp
E6 → E7	160 bp	160 bp	160 bp
E1X → E3	152 bp	No amplification	152 bp ~ 220 bp
E1X → E5b	554 bp 620 bp	N.D	554 bp 620 bp
E5b	234 bp	N.D	234 bp
E3 → E5b	429 bp 495 bp	N.D	429 bp 495 bp
E5b → E7	416 bp	N.D	416 bp

Regions covering B lymphocytes or predicted Pou2f2 isoforms (exons E1 or E1X to E17) were amplified by RT-PCR from B lymphocyte or embryonic spinal cord RNA.
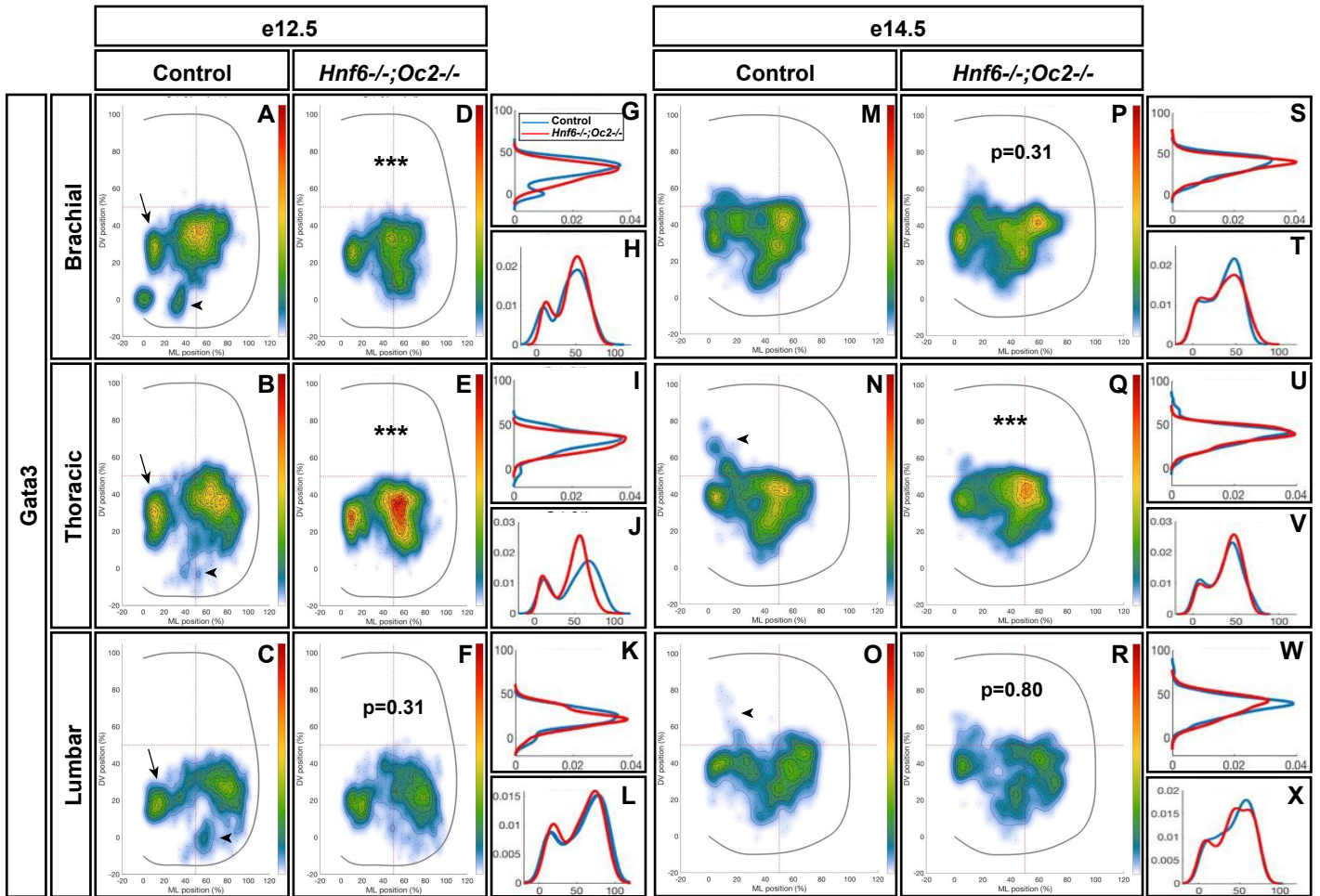Orange cells = unexpected results.
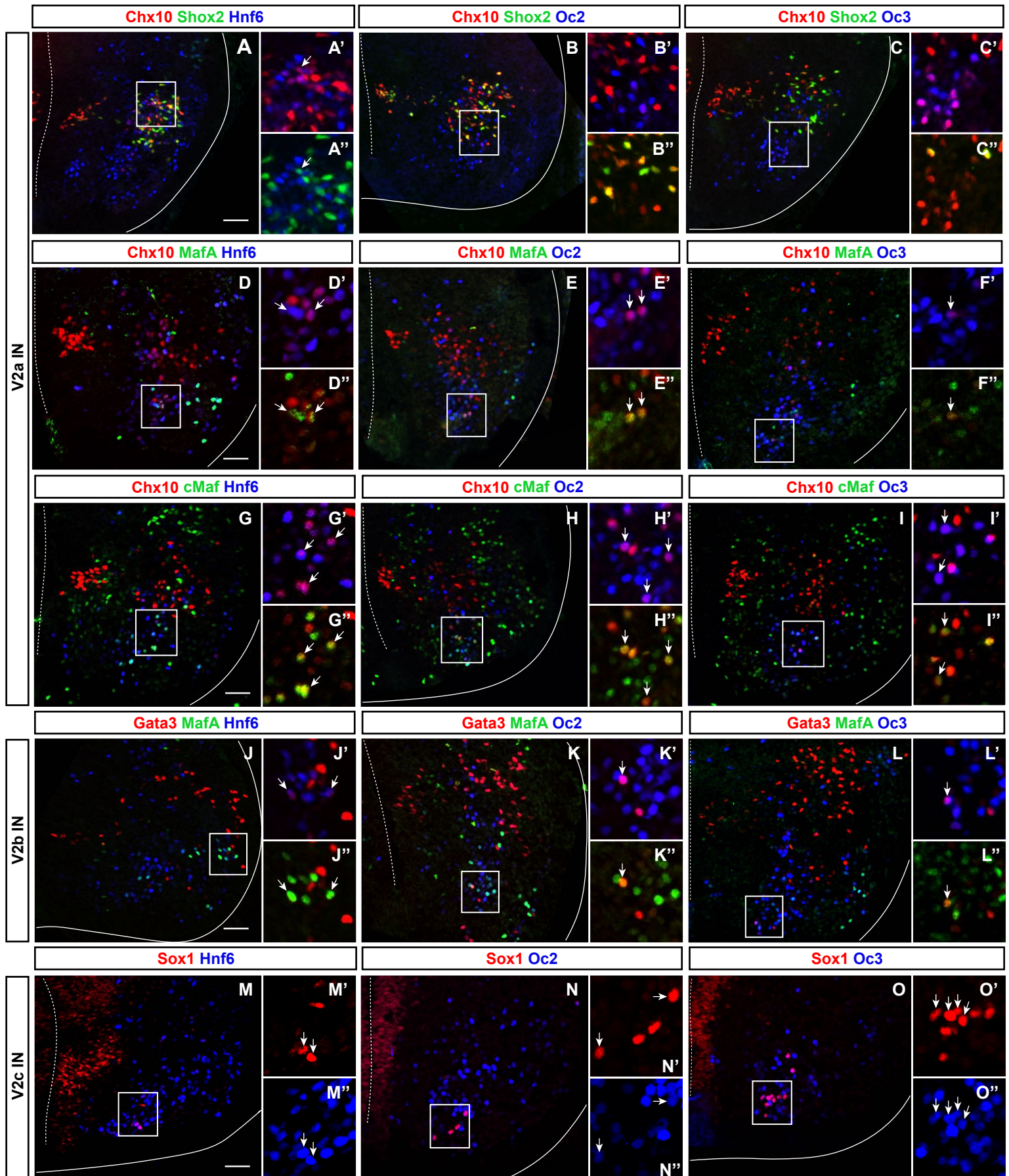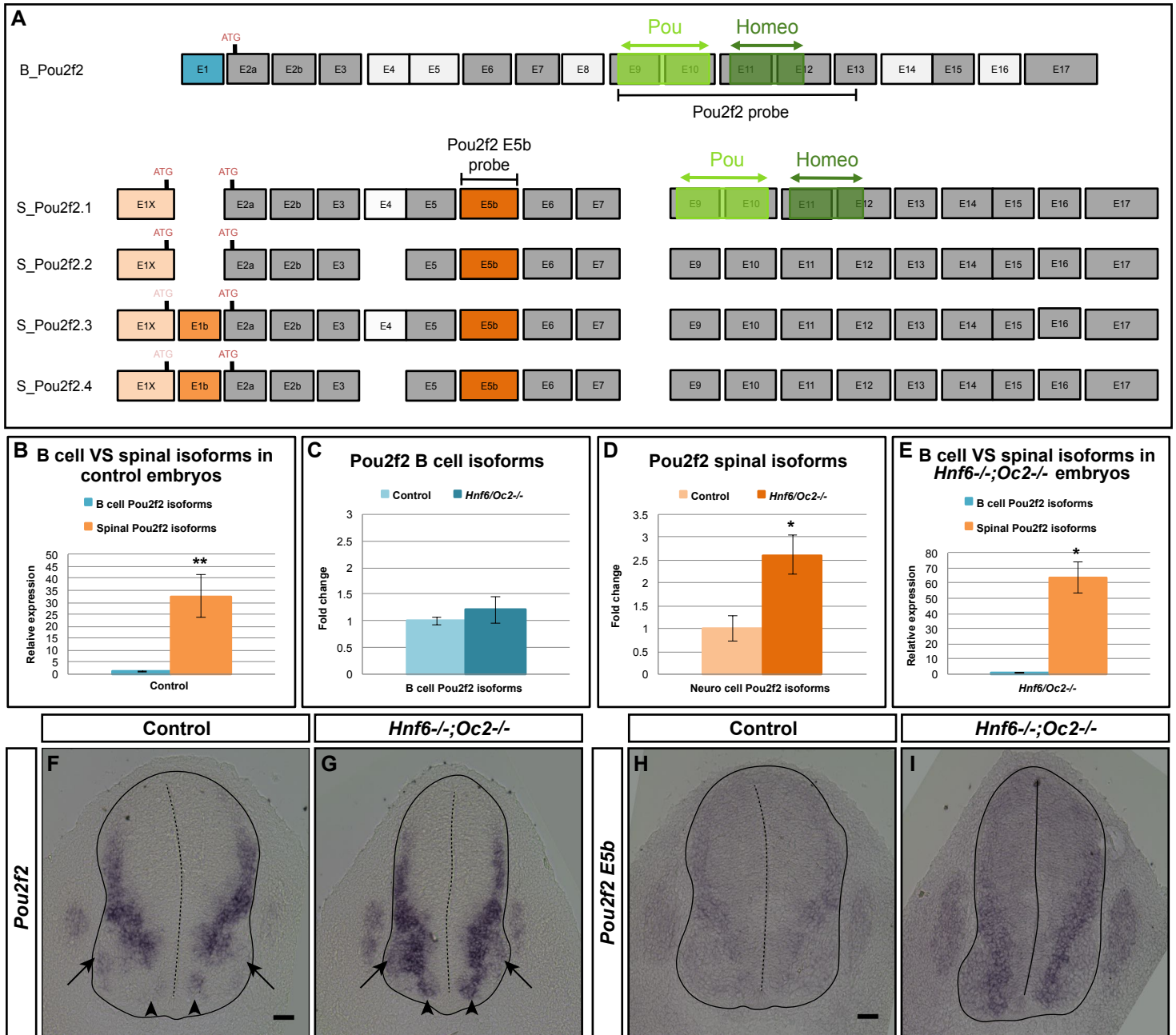
Harris A. et al, Figure 1
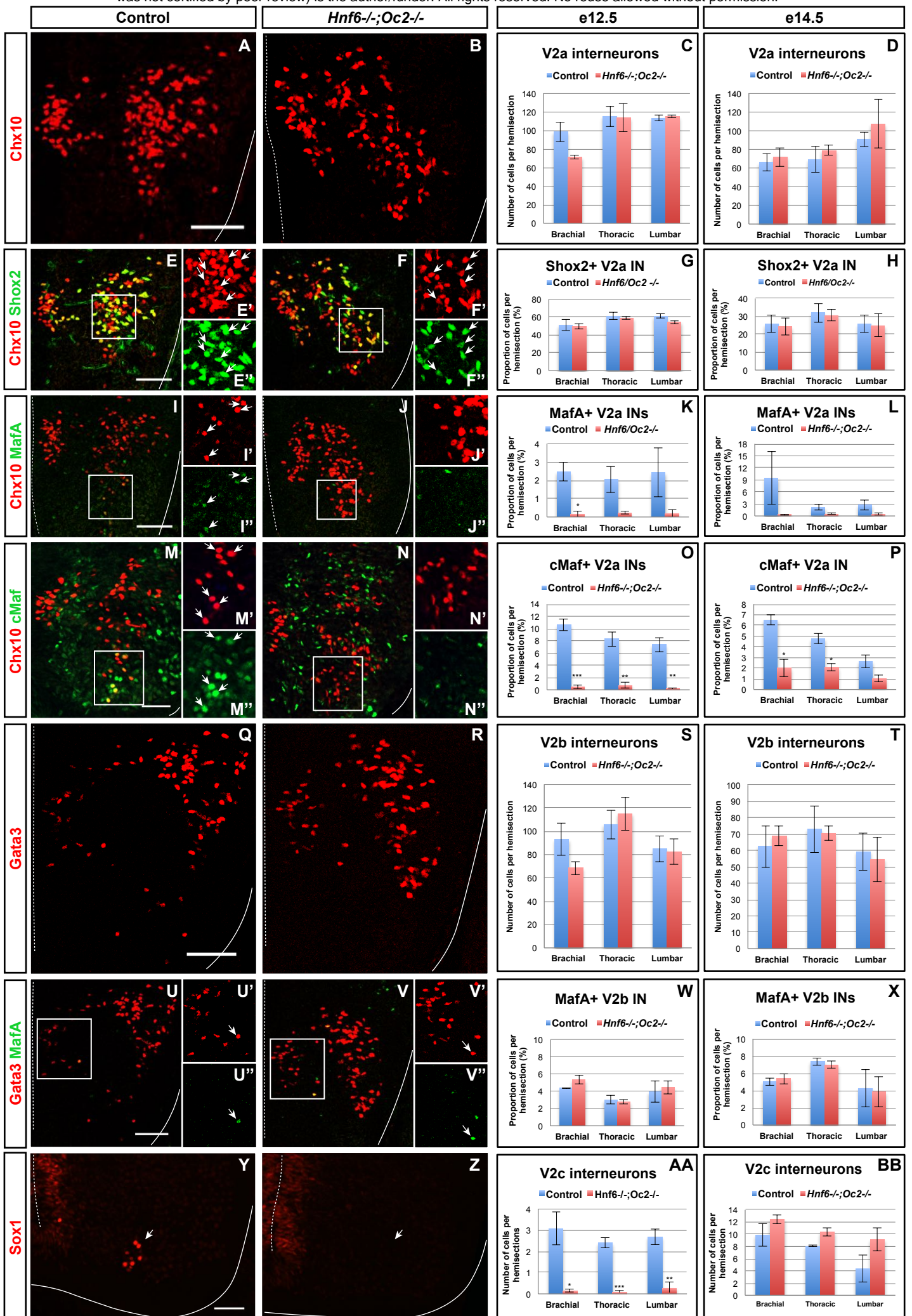
Harris A. et al., Figure 2
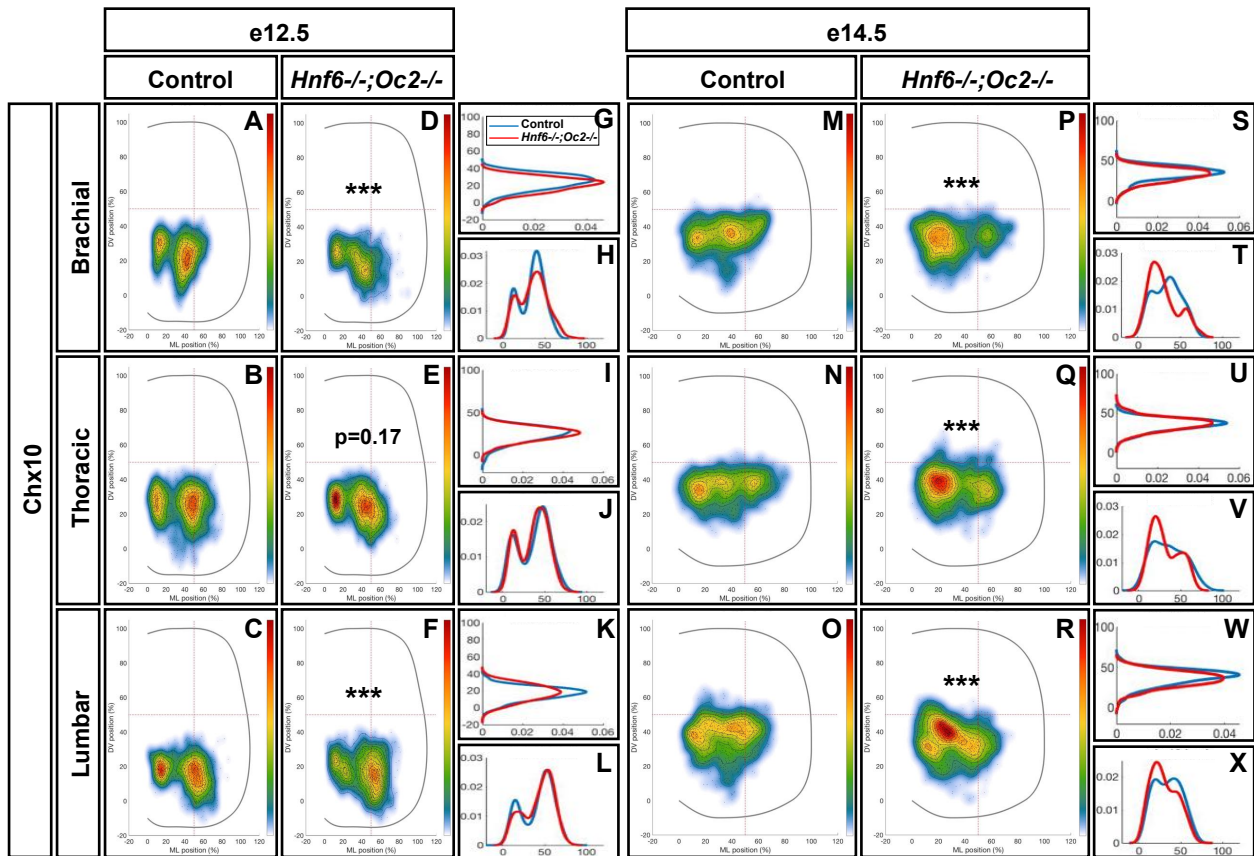
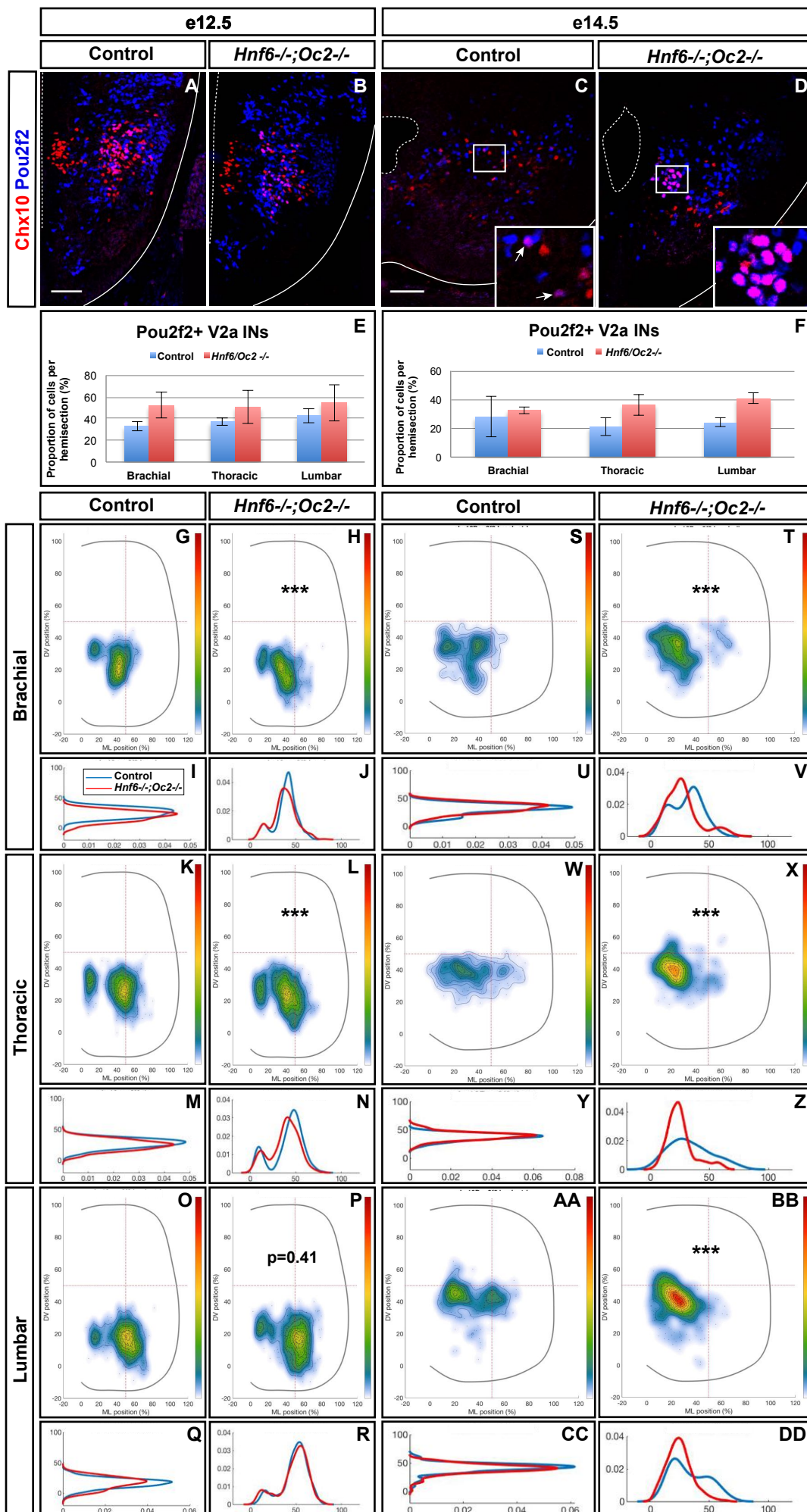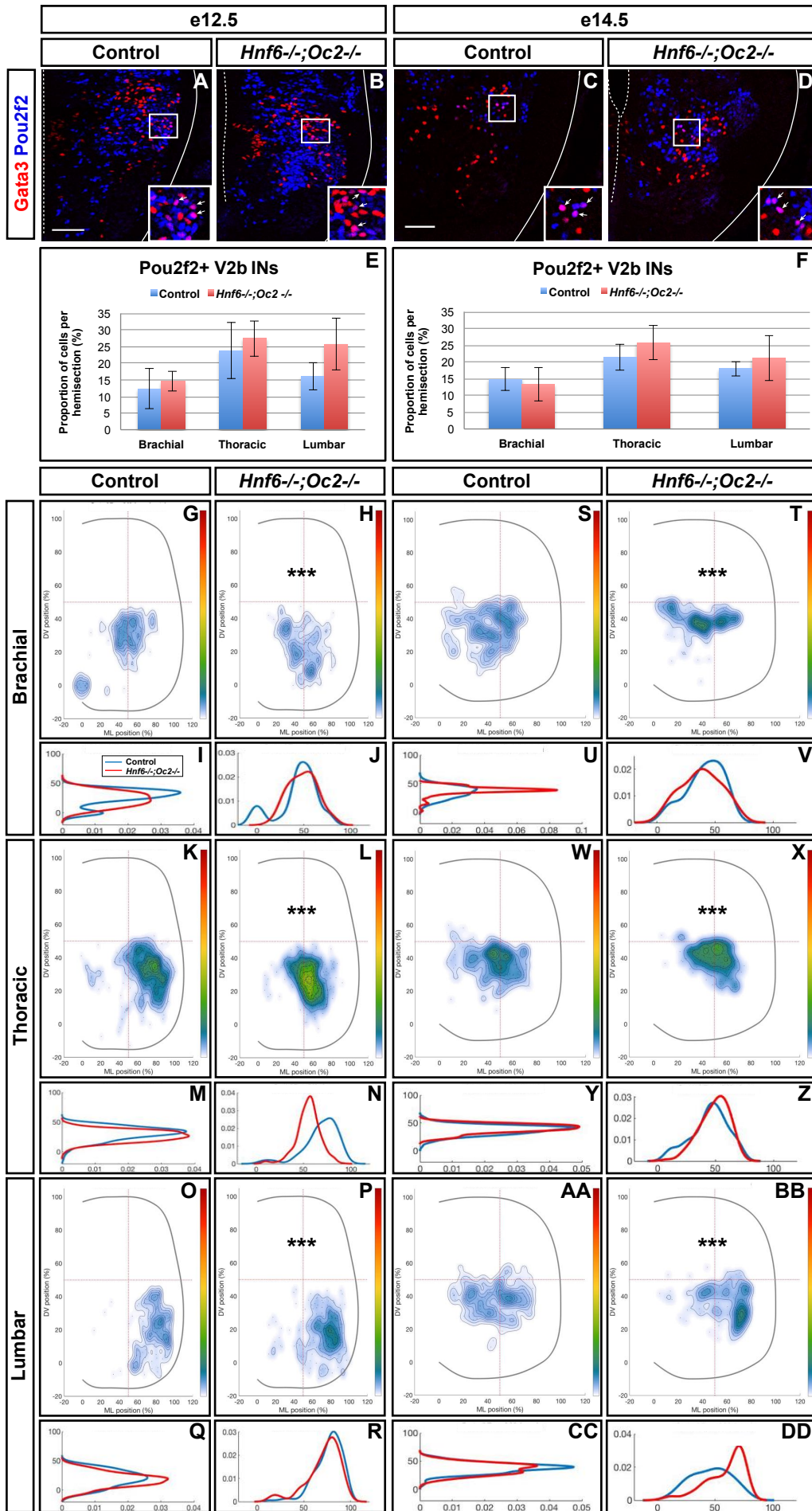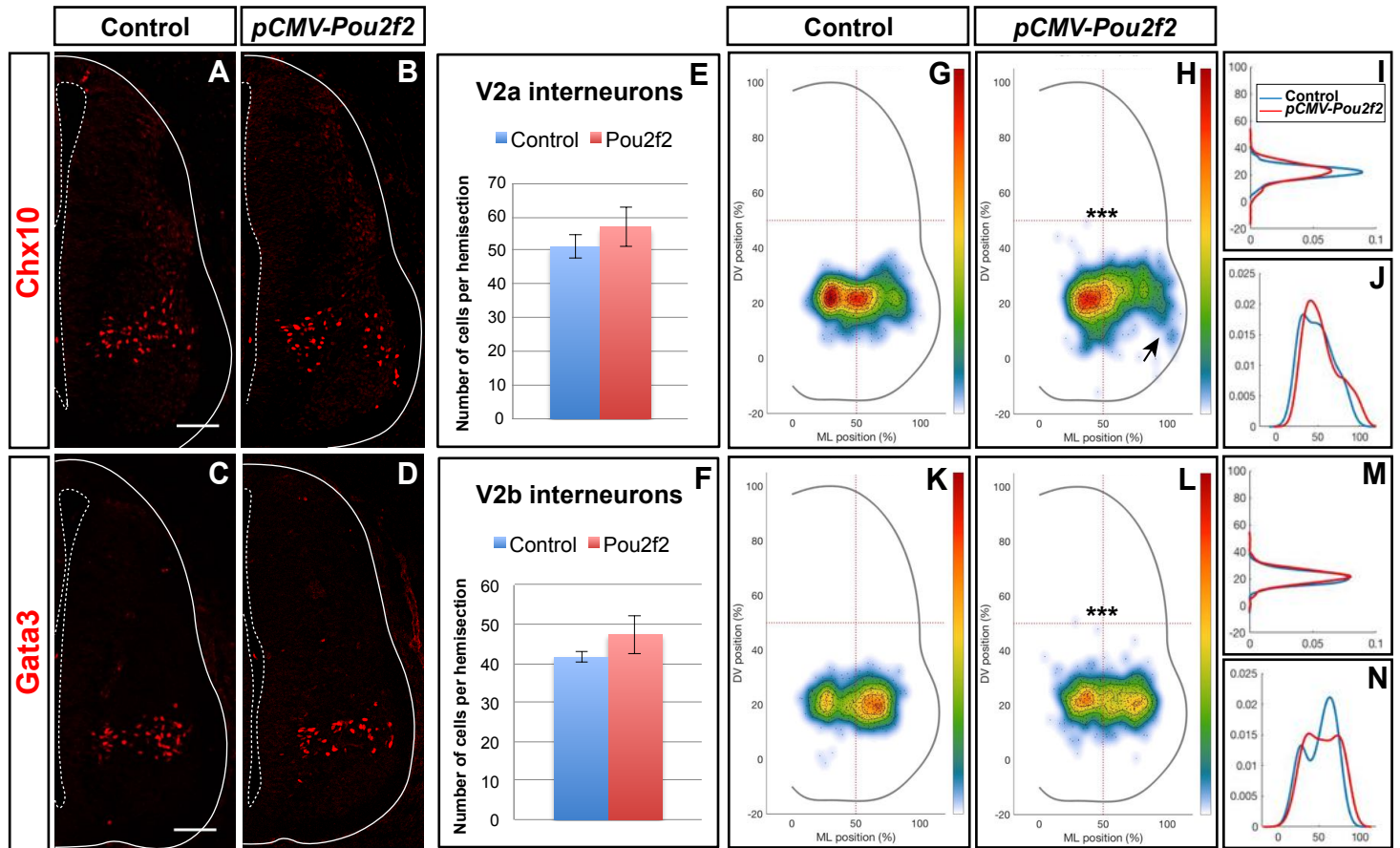**Harris A. et al, Figure 3**

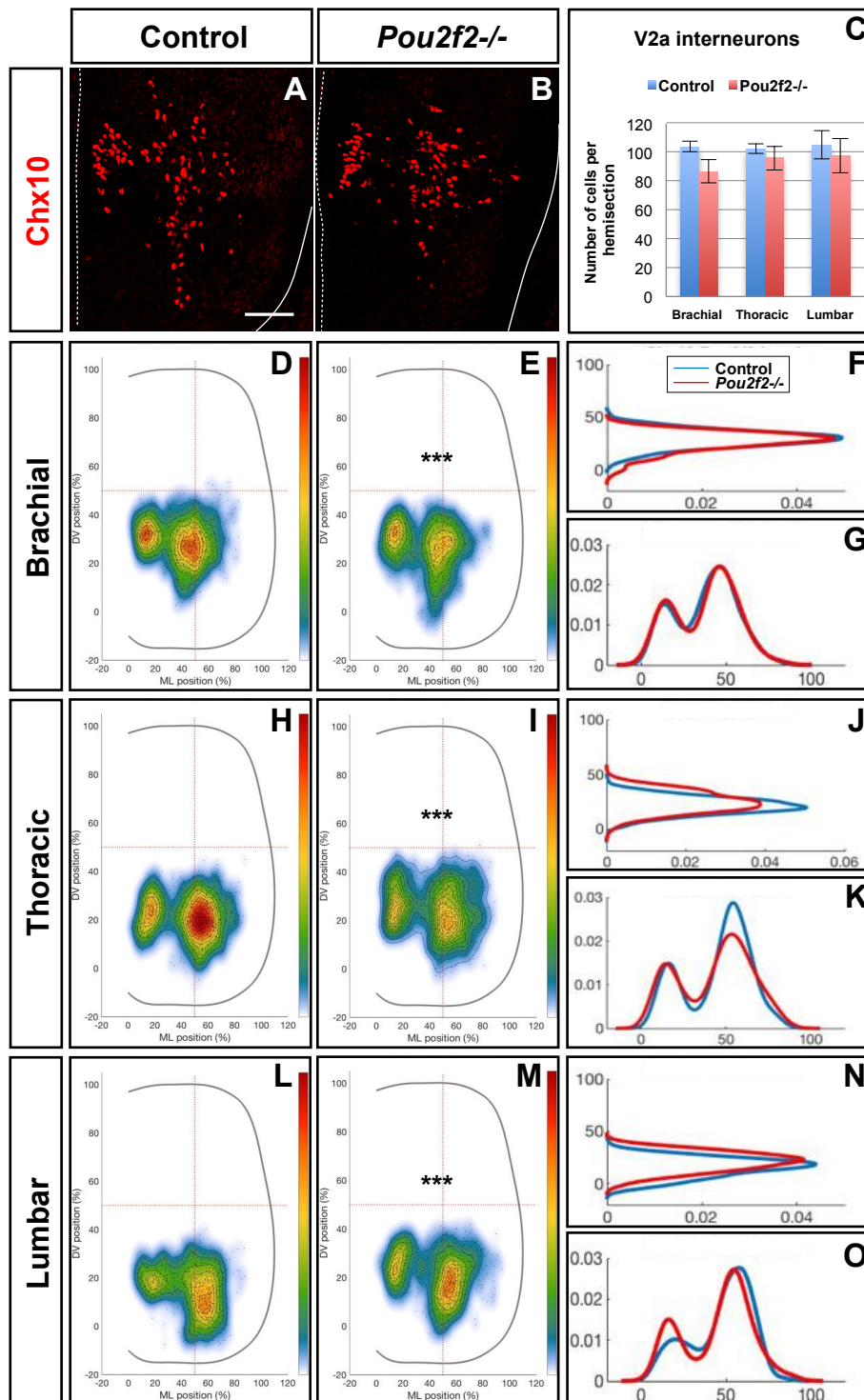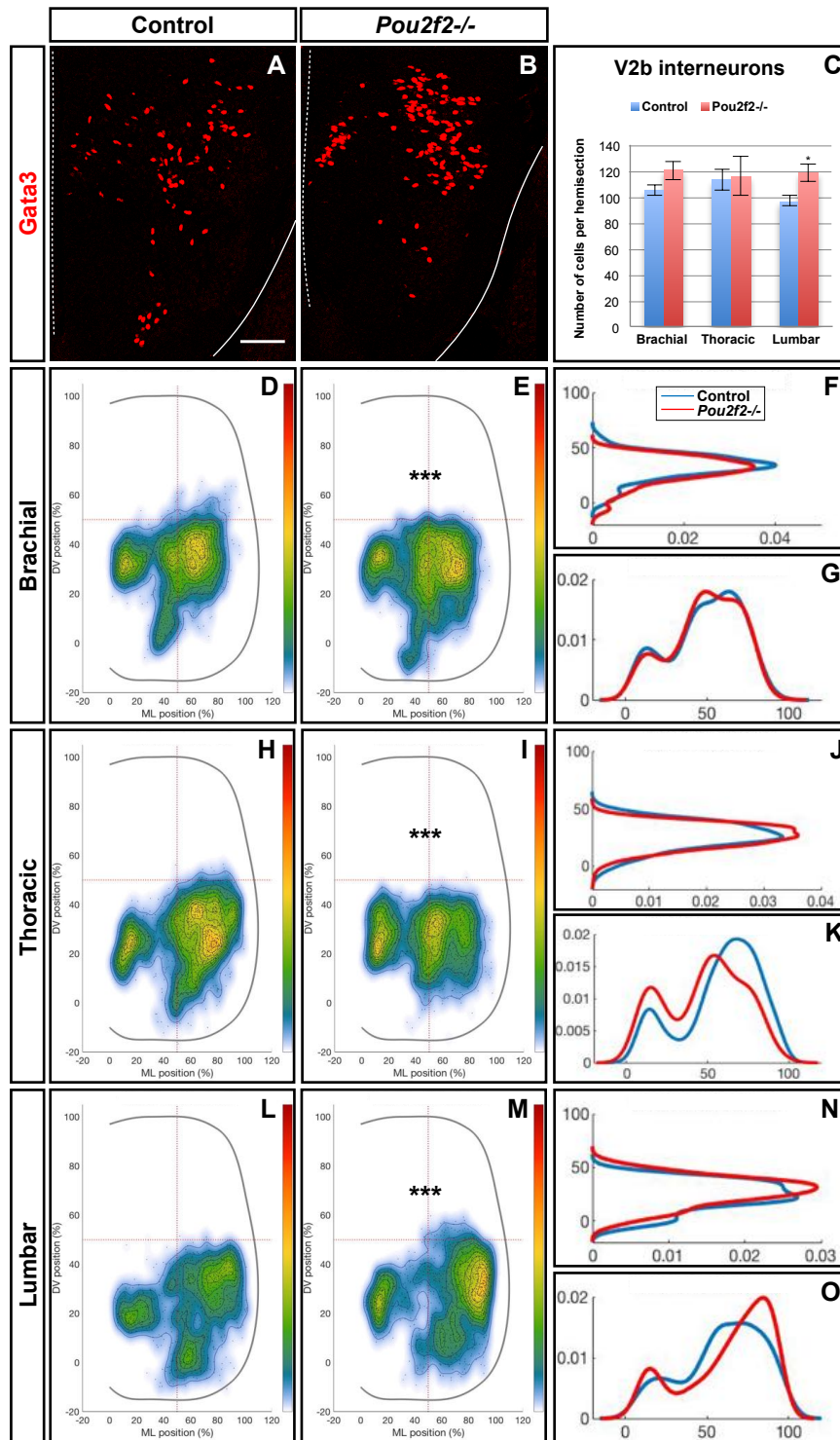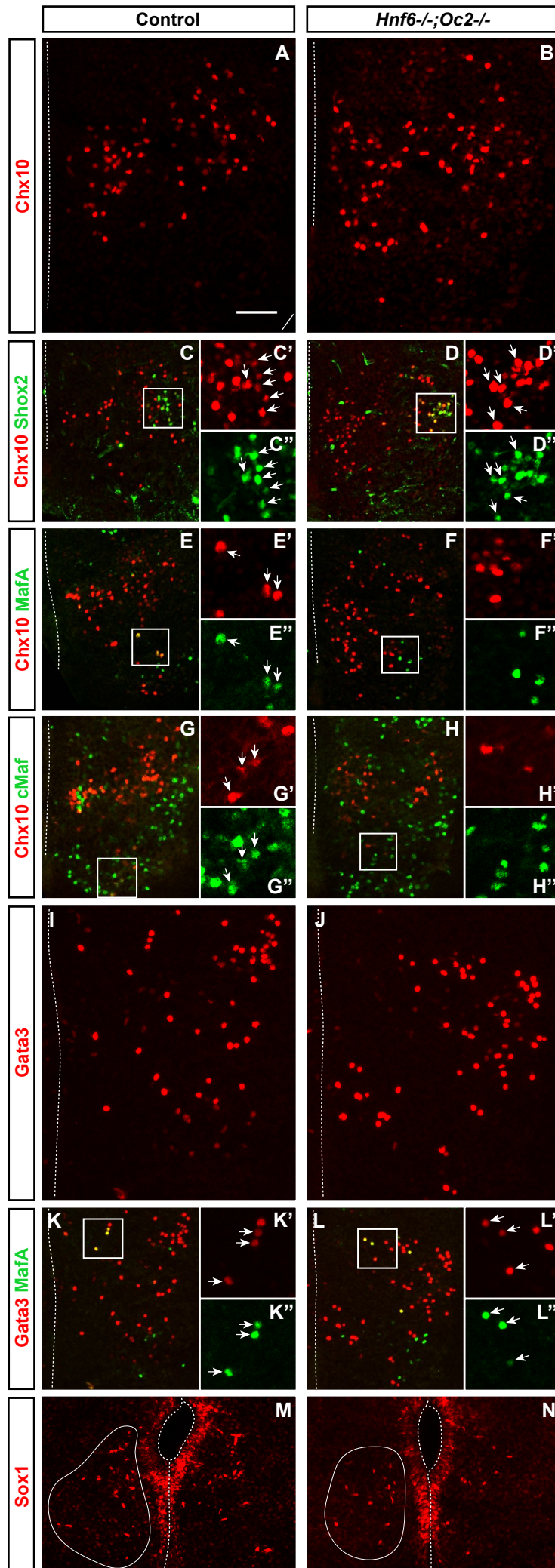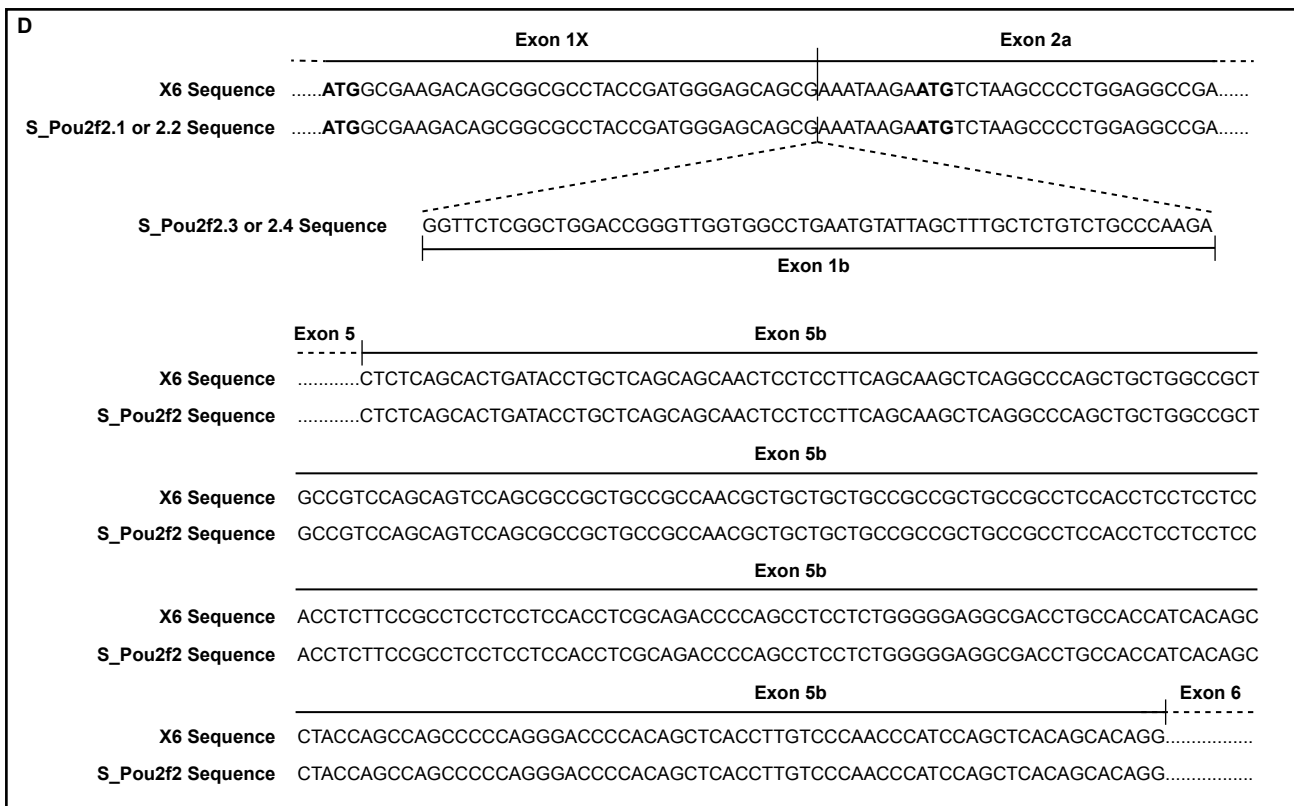**Harris A. et al, Figure 4**

Harris A. et al, Figure 5

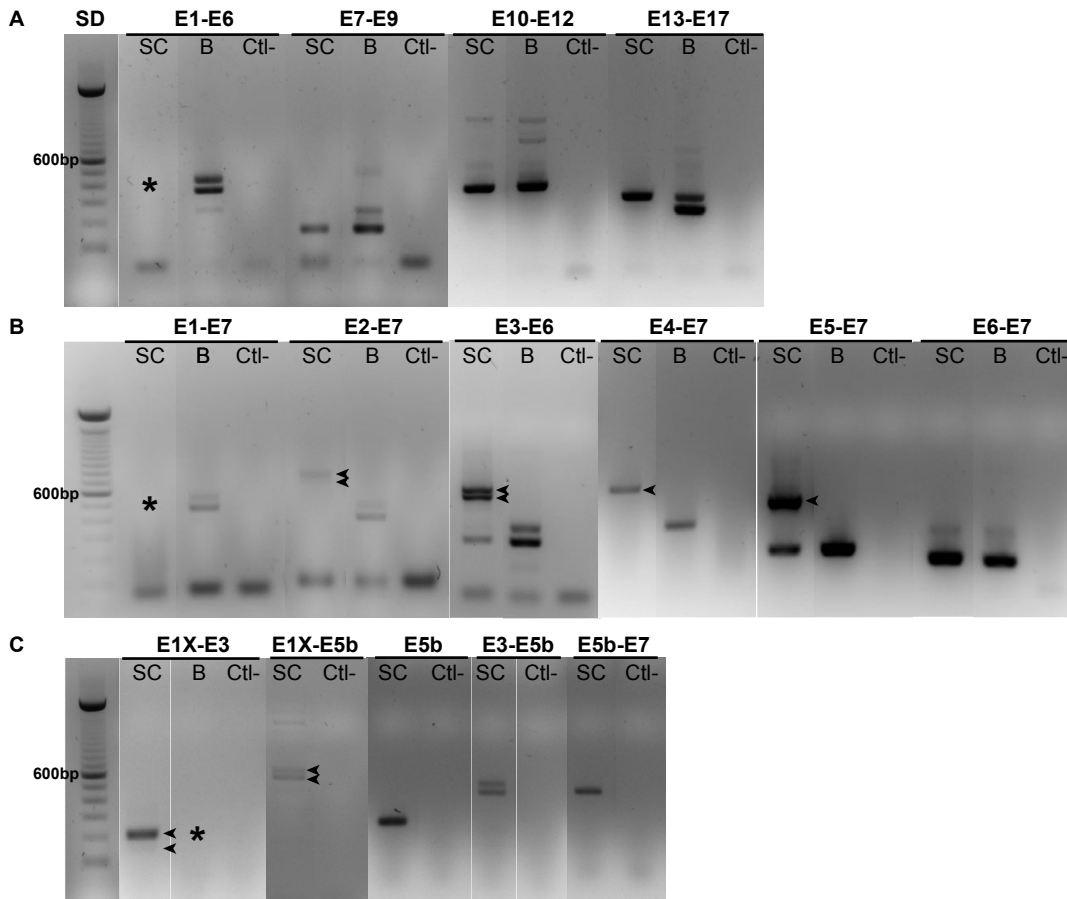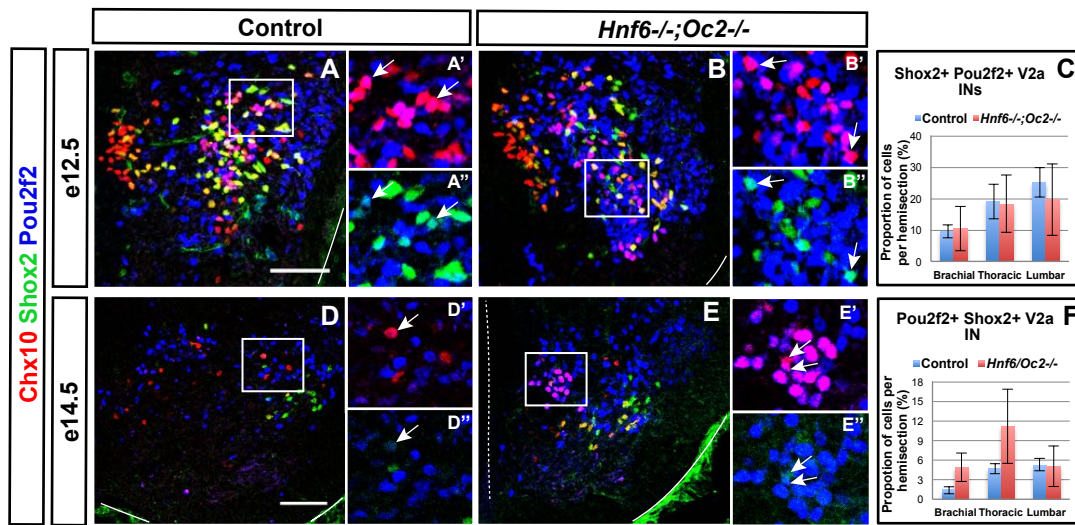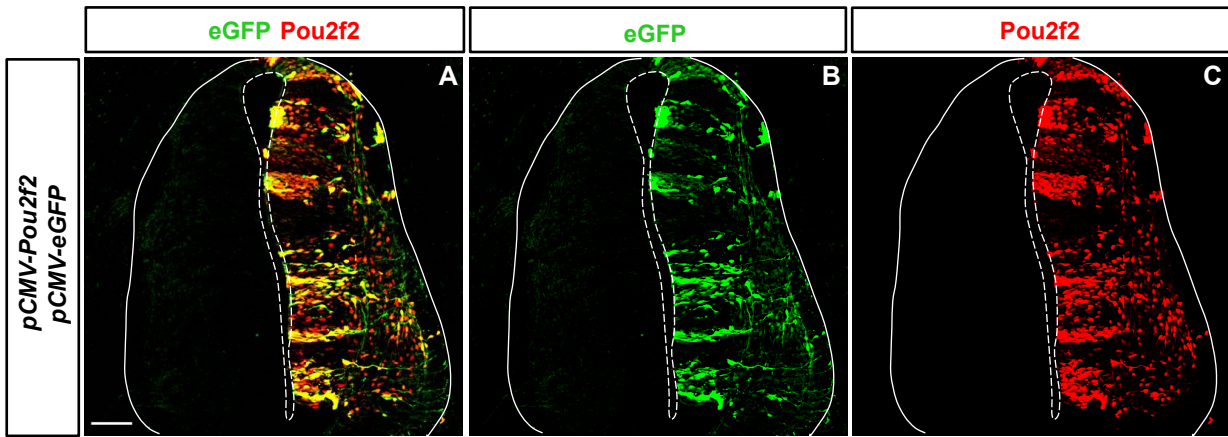Harris A. et al, Figure 6

Harris A. et al, Figure 7

Harris A. et al., Figure 8

Harris A. et al, Figure 9

Harris A. et al, Figure 10

Harris A. et al., Supplementary figure 1

D

	Exon 1X	Exon 2a

X6 Sequence ......**ATG**GCGAAGACAGCGGCGCCTACCGATGGGAGCAGCG|AAATAAGA**ATG**TCTAAGCCCCTGGAGGCCGA......

S_Pou2f2.1 or 2.2 Sequence ......**ATG**GCGAAGACAGCGGCGCCTACCGATGGGAGCAGCG AAATAAGA**ATG**TCTAAGCCCCTGGAGGCCGA......

S_Pou2f2.3 or 2.4 Sequence GGTTCTCGGCTGGACCGGGTTGGTGGCCTGAATGTATTAGCTTTGCTCTGTCTGCCCAAGA

Exon 1b

Exon 5 / Exon 5b

X6 Sequence ............CTCTCAGCACTGATACCTGCTCAGCAGCAACTCCTCCTTCAGCAAGCTCAGGCCCAGCTGCTGGCCGCT

S_Pou2f2 Sequence ............CTCTCAGCACTGATACCTGCTCAGCAGCAACTCCTCCTTCAGCAAGCTCAGGCCCAGCTGCTGGCCGCT

Exon 5b

X6 Sequence GCCGTCCAGCAGTCCAGCGCCGCTGCCGCCAACGCTGCTGCTGCCGCCGCTGCCGCCTCCACCTCCTCCTCC

S_Pou2f2 Sequence GCCGTCCAGCAGTCCAGCGCCGCTGCCGCCAACGCTGCTGCTGCCGCCGCTGCCGCCTCCACCTCCTCCTCC

Exon 5b

X6 Sequence ACCTCTTCCGCCTCCTCCTCCACCTCGCAGACCCCAGCCTCCTCTGGGGGAGGCGACCTGCCACCATCACAGC

S_Pou2f2 Sequence ACCTCTTCCGCCTCCTCCTCCACCTCGCAGACCCCAGCCTCCTCTGGGGGAGGCGACCTGCCACCATCACAGC

Exon 5b / Exon 6

X6 Sequence CTACCAGCCAGCCCCCAGGGACCCCACAGCTCACCTTGTCCCAACCCATCCAGCTCACAGCACAGG.................

S_Pou2f2 Sequence CTACCAGCCAGCCCCCAGGGACCCCACAGCTCACCTTGTCCCAACCCATCCAGCTCACAGCACAGG.................
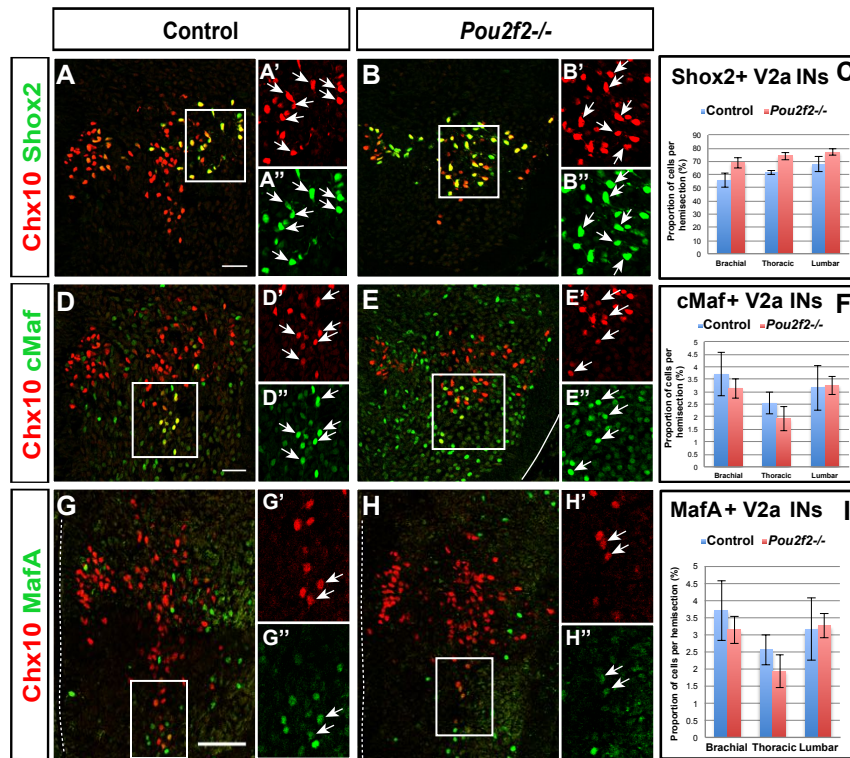
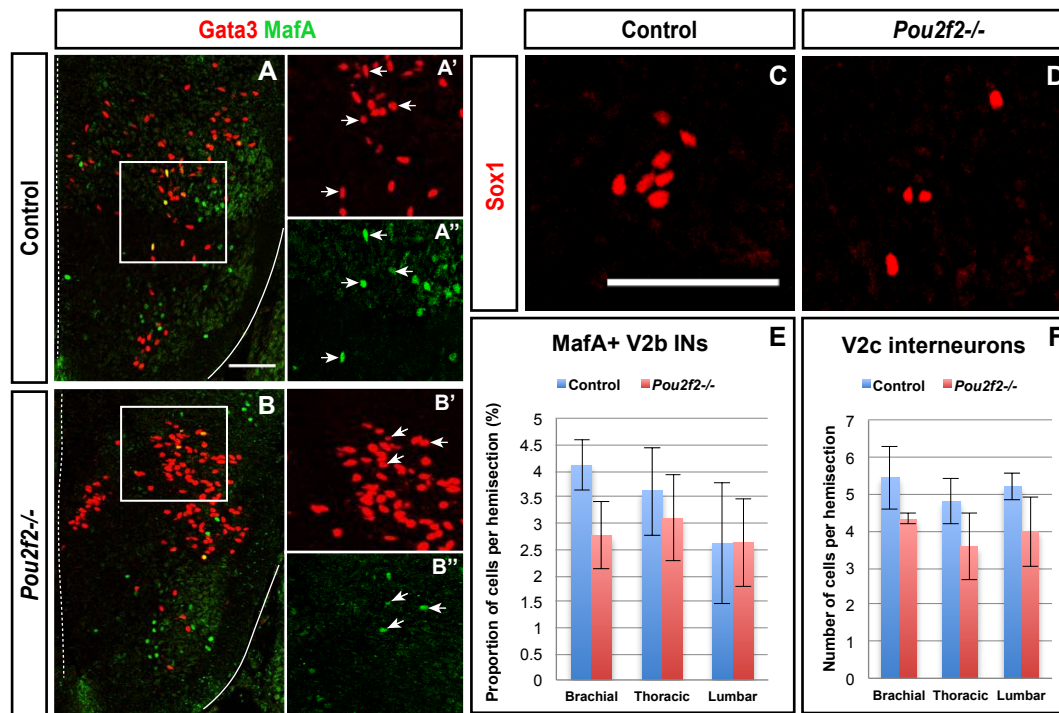**Harris et al., Supplementary figure 2**

Harris A. et al, Supplementary figure 3

Harris A. et al, supplementary figure 4

Harris A. et al, Supplementary figure 5

Harris A. et al., Supplementary figure 6